AD-A038 598 UNITED TECHNOLOGIES RESEARCH CENTER EAST HARTFORD CONN F/G 21/2
DEVELOPMENT OF A THREE-DIMENSIONAL COMBUSTOR FLOW ANALYSIS. VOL--ETC(U)
JUL 75 H J GIBELING, H MCDONALD, W R BRILEY F33615-74-C-2028
UNCLASSIFIED AFAPL-TR-75-59-VOL-1 NL

| OF |
AD A038598

END
DATE FILMED
5-77

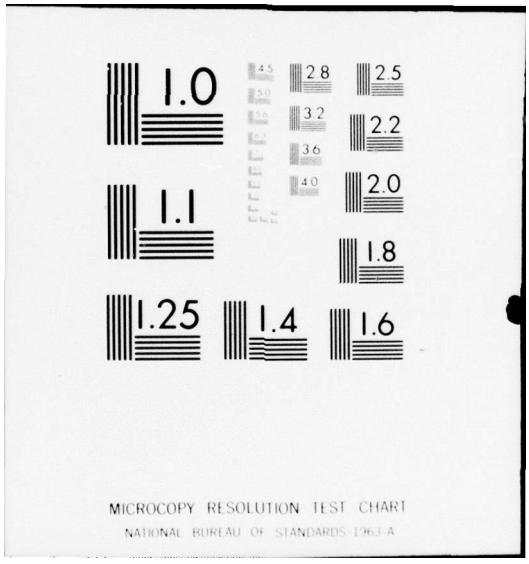
1.0
1.1
1.25
1.4
1.6
1.8
2.0
2.2
2.5
2.8
3.2
3.6
4.0
4.5
5.0
MICROCOPY RESOLUTION TEST CHART
NATIONAL BUREAU OF STANDARDS-1963-A

AFAPL-TR-75-59
Volume I

(18)

DEVELOPMENT OF A THREE-DIMENSIONAL COMBUSTOR FLOW ANALYSIS
Volume I: Theoretical Studies

UNITED TECHNOLOGIES RESEARCH CENTER
EAST HARTFORD, CONNECTICUT 06108

JULY 1975

TECHNICAL REPORT AFAPL-TR-75-59, Volume I
INTERIM REPORT FOR PERIOD 1 MARCH 74 - 1 JUNE 75

AIR FORCE AERO-PROPULSION LABORATORY
AIR FORCE WRIGHT AERONAUTICAL LABORATORIES
AIR FORCE SYSTEMS COMMAND
WRIGHT-PATTERSON AIR FORCE BASE, OHIO 45433

NOTICE

When Government drawings, specifications, or other data are used for any purpose other than in connection with a definitely related Government procurement operation, the United States Government thereby incurs no responsibility nor any obligation whatsoever; and the fact that the Government may have formulated, furnished, or in any way supplied the said drawings, specifications, or other data, is not to be regarded by implication or otherwise as in any manner licensing the holder or any other person or corporation, or conveying any rights or permission to manufacture, use, or sell any patented invention that may in any way be related thereto.

This final report was submitted by United Technologies Research Center, under Contract F33615-74-C-2028. The effort was sponsored by the Air Force Aero-Propulsion Laboratory, Air Force Systems Command, Wright-Patterson AFB, Ohio, under Project 3066, Task 306605 and Work Unit 30660529 with Dale A. Hudson, AFAPL/TBC, as Project Engineer. Henry McDonald of United Technologies Research Center was technically responsible for the work.

The authors wish to acknowledge the helpful comments and criticisms of Dr. S. J. Shamroth and Mr. R. C. Buggeln during the development of this procedure. The authors also wish to acknowledge the unpublished experimental data provided by Hratch Semerjian of Pratt & Whitney Aircraft and taken under the Basic Technology Program.

This report has been reviewed by the Information Office, (ASD/OIP) and is releasable to the National Technical Information Service (NTIS). At NTIS, it will be available to the general public, including foreign nations.

This technical report has been reviewed and is approved for publication.

Dale A. Hudson

DALE A. HUDSON, GS-09
Project Engineer

FOR THE COMMANDER

Robert E. Henderson

ROBERT E. HENDERSON
Tech Area Manager, Combustion

Copies of this report should not be returned unless return is required by security considerations, contractual obligations, or notice on a specific document.

UNCLASSIFIED

SECURITY CLASSIFICATION OF THIS PAGE (When Data Entered)

REPORT DOCUMENTATION PAGE

READ INSTRUCTIONS BEFORE COMPLETING FORM

1. REPORT NUMBER: AFAPL-TR-75-59 Volume I

2. GOVT ACCESSION NO.

3. RECIPIENT'S CATALOG NUMBER

4. TITLE (and Subtitle): DEVELOPMENT OF A THREE-DIMENSIONAL COMBUSTOR FLOW ANALYSIS. VOLUME I. THEORETICAL STUDIES.

5. TYPE OF REPORT & PERIOD COVERED: Interim Report, 1 Mar 1974 — 1 Jul 1975.

6. PERFORMING ORG. REPORT NUMBER

7. AUTHOR(s): Howard J. Gibeling, Henry McDonald, W. Roger Briley

8. CONTRACT OR GRANT NUMBER(s): F33615-74-C-2028

9. PERFORMING ORGANIZATION NAME AND ADDRESS: United Technologies Research Center, 400 Main Street, East Hartford, Connecticut 06108

10. PROGRAM ELEMENT, PROJECT, TASK AREA & WORK UNIT NUMBERS: Project 3066, Task 306605, Work Unit 30660529

11. CONTROLLING OFFICE NAME AND ADDRESS: United States Air Force, Air Force Systems Command, Hq. 4950th Test Wing 4950/PMNB, Wright Patterson AFB, Ohio 45433

12. REPORT DATE: Jul 1975

13. NUMBER OF PAGES: 70

14. MONITORING AGENCY NAME & ADDRESS (if different from Controlling Office): Air Force Aero-Propulsion Laboratory, Air Force Wright Aeronautical Laboratories, Air Force Systems Command, Wright-Patterson AFB, Ohio 45433

15. SECURITY CLASS. (of this report): UNCLASSIFIED

15a. DECLASSIFICATION/DOWNGRADING SCHEDULE

16. DISTRIBUTION STATEMENT (of this Report): Approved for public release; Distribution unlimited. 80 p.

17. DISTRIBUTION STATEMENT (of the abstract entered in Block 20, if different from Report)

16) 3066 17) 05 18) AFAPL

18. SUPPLEMENTARY NOTES

19) TR-75-59-Vol-I

19. KEY WORDS (Continue on reverse side if necessary and identify by block number)

20. ABSTRACT (Continue on reverse side if necessary and identify by block number)

A three-dimensional computational procedure is presented for calculating the coupled flow and chemistry within rectangular or axisymmetric combustors with a discrete circumferential distribution of injection ports. The compressible time-averaged Navier-Stokes equations are solved with coupled pseudo-kinetic hydrocarbon chemistry including the effects of turbulence, droplet vaporization and burning, and radiation transport. An eddy viscosity →

next page

DD FORM 1 JAN 73 1473 EDITION OF 1 NOV 65 IS OBSOLETE

SECURITY CLASSIFICATION OF THIS PAGE (When Data Entered)

409252

cont

~~turbulence model with an ad-hoc specified mixing length distribution is~~ employed at present. The governing equations are solved using the Multidimensional Implicit Nonlinear Time-dependent (MINT) procedure, which employs a unique linearization technique and a Douglas-Gunn alternating-direction-implicit (ADI) scheme. Calculations were made for the flow in a rectangular combustion chamber with a discrete distribution of inlet injection ports and the results are compared with the experimental data available for this configuration.

TABLE OF CONTENTS

LIST OF ILLUSTRATIONS

SYMBOLS

Symbol	Description
a	Coefficient in wall function, Eq. (14b)
A_j	Chemical rate constant frequency factor, Eq. (28)
$\bar{\bar{A}}^n$	Square matrix containing time derivative coefficients, Eq. (80)
B_j	Chemical activation energy, Eq. (28)
Bo	Boltzmann number, Bo = $\rho_D U_D h_D / q_{R_D}$
c_p	Specific heat of mixture at constant pressure, nondimensional
c_{p_i}	Specific heat of species i, nondimensional
c_1, c_2	Coefficients in wall function, Eq. (14)
C_i	Concentration of species i, moles per unit volume
$\bar{\bar{D}}_1^n$, $\bar{\bar{D}}_2^n$, $\bar{\bar{D}}_3^n$	Square matrices containing spatial difference operators for x_1, x_2, x_3 directions, Eq. (80)
$\bar{\bar{e}}$	Mean flow rate of strain tensor, Eq. (6)
f_j	Time-averaged particle fraction for class (j)
f_o	Mass fraction of O_2 in oxidizer (f_o = 0.2322 for air)
G_i	Radiation flux function, Eq. (55); nondimensional
h	Static enthalpy of mixture
h_c	Heat of combustion of fuel
h_i	Static enthalpy of species i, Eq. (9); nondimensional
h_i^f	Heat of formation of species i, nondimensional
h_v	Heat of vaporization of liquid fuel

h_1, h_2, h_3	Metric coefficients for coordinates x_1, x_2, x_3
H	Time-averaged stagnation enthalpy of mixture, Eq. (8); nondimensional
$\vec{i}_1$, $\vec{i}_2$, $\vec{i}_3$	Unit vectors in coordinate directions x_1, x_2, x_3
k_j	Arrenhius rate constant, Eq. (28)
k_f, k_b	Forward and backward chemical rate constants
k_{HC}	Hydrocarbon chemistry rate constant, Eq. (36); nondimensional
ℓ	Mixing length, Eq. (13); nondimensional
L	Reference length, dimensional
$\dot{m}$	Droplet vaporization rate, Eq. (49); nondimensional
$\bar{m}_d$	Droplet vaporization rate function, Eq. (50); nondimensional
m_i	Time-averaged mass fraction of species i
m_i^*	Time-averaged mass fraction of species i in nonreacting flow
m_N	Mass fraction of inert species, Eq. (34)
m_p	Mass fraction of combustion products, Eq. (35)
m_{HC}	Mass fraction of fuel which has reacted, Eq. (42)
m_{O_2}	Mass fraction of O_2 which has reacted, Eq. (43)
n	Normal coordinate at a surface
N	Number of grid points in a given coordinate direction
N_j	Chemical rate constant exponent, Eq. (28)
p	Time-averaged static pressure, Eq. (7a); nondimensional
Pr	Prandtl number

Pr_{eff}	Effective turbulent Prandtl number
q_i^+, q_i^-	Radiation fluxes in the positive and negative x_i - coordinate direction, nondimensional
q_{in}	Incoming normal radiation flux component at a surface, nondimensional
$\vec{q}_R$	Radiation flux vector, nondimensional
Q_i	Net radiation flux in x_i coordinate direction, Eq. (56); nondimensional
r	Droplet radius or radial coordinate (Fig. 1)
r_i	Chemical production rate term, i^{th} species equation; nondimensional
r_j	Lower radius of j^{th} particle fraction class, nondimensional
r_o	Pipe radius or duct half-width, Eq. (13); nondimensional
R_g	Universal gas constant
R_j	Droplet source term, j^{th} particle class; nondimensional
R_s	Stoichiometric ratio, Eq. (33)
Re	Reference Reynolds number, $Re = \rho_D U_D L/\mu_D$
$Re_{\Delta x_i}$	Mesh Reynolds number for x_i coordinate direction, nondimensional
s_1, s_2	Tangential coordinates at a surface
$s_{i,j}$	Droplet vaporization source term, i^{th} species equation and j^{th} particle fraction class; nondimensional
$\bar{S}^n$	Vector containing known n-level quantities appearing as source terms in difference equation, Eq. (80)
Sc	Schmidt number
Sc_{eff}	Effective turbulent Schmidt number

SYMBOLS (Continued)

t	Time, nondimensional
$\overline{\overline{t}}$	General tensor, Appendix A
T	Time-averaged static temperature, nondimensional
T_b	Boiling temperature of liquid fuel, nondimensional
T_w	Wall surface temperature, nondimensional
$\vec{u}$	Time-averaged velocity vector, nondimensional $\vec{u} = (u, v, w)$
u, v, w	Time-averaged x_1, x_2, and x_3 velocity components, nondimensional
$\tilde{u}$	Total tangential velocity component at a wall, nondimensional
u^+	Wall function velocity, Eq. (15); nondimensional
u^*	Friction velocity, Eq. (17); nondimensional
U_D	Reference velocity, dimensional
$\vec{v}$	General vector, Appendix A
W_D	Reference molecular weight, gm/mole
W_i	Molecular weight of species i, nondimensional
W_m	Mixture molecular weight, Eq. (7b); nondimensional
x_1, x_2, x_3	Orthogonal curvilinear coordinates, see Fig. 1 and Appendix A; nondimensional
X_T	Transformed coordinate variable, Eq. (89); nondimensional
y	Distance to nearest wall for mixing length, Eq. (13); nondimensional
y^+	Wall function coordinate, Eq. (16); nondimensional
Z	Reciprocal mixture molecular weight, Eq. (7b); nondimensional

α_a	Radiation flux absorption coefficient, Eqs. (53-54); nondimensional
α_a'	Actual radiation absorption coefficient, nondimensional
α_p	Planck mean absorption coefficient
α_R	Rosseland mean absorption coefficient
α_s	Radiation flux scattering coefficient, Eqs. (53-54); nondimensional
α_ν'	Actual frequency dependent absorption coefficient
β	Grid transformation parameter, Eq. (89)
Γ_m, Γ_h, Γ_p	Effective turbulent exchange coefficients for mass, enthalpy and droplet transport
δ_k	Spatial difference operators for central difference approximation to first derivatives (k = 1,2,3), Eq. (74)
δ_k^2	Spatial difference operators for central difference approximation to second derivatives (k = 1,2,3), Eq. (75)
Δx_1, Δx_2, Δx_3	Grid spacings for the x_1, x_2, x_3 directions
Δt	Time step
ϵ_i	Artificial viscosity for x_i direction
ϵ_w	Wall emissivity
ϕ	Dummy symbol for any dependent variable
$\bar{\phi}$	Dummy vector symbol for dependent variables
Φ	Time-averaged hybrid species mass fraction, Eq. (32)
μ_{lam}	Laminar dynamic viscosity, nondimensional
μ_{eff}	Effective turbulent viscosity, nondimensional

SYMBOLS (Concluded)

ν_2	Moles of O_2 in reaction, Eq. (29)
ρ	Time-averaged density, nondimensional
ρ_d	Liquid droplet (fuel) density, nondimensional
σ	Stefan-Boltzmann constant, dimensional
τ_ν	Frequency dependent optical depth, Eq. (62); nondimensional
τ_w	Wall shear stress, nondimensional; see Eq. (17)

SUBSCRIPTS

D	Denotes dimensional reference value
e	Denotes chemical equilibrium
g	Gaseous or gas phase
i, j, k	Grid point indices; x_1, x_2, x_3 directions
n	Normal direction at a surface
NO	Denotes nitric oxide species
p	Denotes combustion products or particle fraction
R	Denotes radiation quantity
1	Denotes fuel (C_nH_m) species
2	Denotes oxidizer (O_2) species

SUPERSCRIPTS

n	Denotes time level (t^n)
T	Denotes matrix or tensor transpose
*	Denotes solution at intermediate step of ADI procedure

SECTION I

INTRODUCTION

Predictions of gas turbine combustor performance and pollutant emission characteristics require modeling procedures possessing a high degree of sophistication. Past attempts at modeling combustion systems have been largely frustrated by the complexity of the coupled hydrodynamic and chemical processes. The difficulty can be largely attributed to the lack of understanding of the flow processes which, through the exchange of heat, mass and momentum, can directly relate to pollutant formation and combustion efficiency. For example, swirling flow has been shown to have an important influence on the stability and combustion intensity of flames (Ref. 1) as well as on residence-time distributions (Ref. 2) in combustors which, in turn, can be related to combustor performance and efficiency as well as to emission characteristics (Refs. 3 and 4). Techniques employed in modeling combustor flow processes have generally been highly simplified, particularly flow modeling techniques where stirred reactor concepts and one-dimensional assumptions are

---

1. Beer, J. M. and N. A. Chigier: Stability and Combustion Intensity of Pulverized Coal Flames - Effect of Swirl and Impingement. Journal of the Institute of Fuel, December 1969.
2. Beer, J. M. and W. Leucker: Turbulent Flames in Rotating Flow Systems. Paper No. Inst. F-NAFTC-7, North American Fuel Technology Conference, Ottawa, Canada, 1970.
3. Beer, J. M. and J. B. Lee: The Effects of Residence Time Distribution on the Performance and Efficiency of Combustors. The Combustion Institute, 1965, pp. 1187-1202.
4. Marteney, P. J.: Analytical Study of the Kinetics of Formation of Nitrogen Oxide in Hydrocarbon - Air Combustion. Combustion Science and Technology, Vol. 1, 1970, pp. 37-45.

employed (Refs. 5 through 10). Chemistry is frequently modeled by assuming equilibrium hydrocarbon fuel decomposition and two phase flow effects are seldom considered. In some more recent modeling attempts, for example, Fletcher and Heywood (Ref. 5) and Hammond and Mellor (Refs. 6 and 7), the stirred reactor concept is employed to assess the effect of residence-time on combustion behavior and to predict pollutant emissions in gas turbines. Droplet vaporization and burning were neglected in these studies; however, a quasi-global finite-rate hydrocarbon combustion mechanism was employed by Hammond and Mellor to model the chemistry. In related work, Roberts, et al., (Ref. 8), in an attempt to predict nitrogen oxide formation in gas turbine combustors, subdivided the combustor into three regions: one corresponding to the central recirculation portion of the upstream zone; a second representing the flow region surrounding the recirculation zone which was interpreted to be a one-dimensional reacting zone; and the third downstream zone modeled as a one-dimensional region. Both finite-rate and equilibrium hydrocarbon chemistry models were considered. It is interesting that little difference in the predicted NO levels was noted in their results between the equilibrium and finite-rate hydrocarbon cases. A more recent analysis directed toward low power application by Mosier, et al., (Ref. 9) basically extended the work of Ref. 8 through the use of a more sophisticated finite-rate hydrocarbon chemistry model obtaining trends in agreement with experimental data. The modular approach proposed by Edelman and Economos (Ref. 10) is an attempt at formulating a general analytical procedure for predicting combustor behavior by treating the various critical combustor processes on an individual basis or coupled as a function of operating conditions. Difficulty with the approach lies with its method of accounting for recirculation (a stirred reactor is presently used) and its inability to provide a unified description of the burner under a given set of operating conditions.

---

5. Fletcher, R. S. and J. B. Heywood: A Model for Nitric Oxide Emission from Aircraft Gas Turbine Engines. AIAA Paper 71-123, 1971.
6. Hammond, D. C., Jr. and A. M. Mellor: Analytical Predictions of Emissions from and Within an Allison J-33 Combustor. Combustion Science and Technology, Vol. 6, 1973, pp. 279-286.
7. Hammond, D. C., Jr. and A. M. Mellor: Analytical Calculations for the Performance and Pollutant Emissions of Gas Turbine Combustors. Combustion Science and Technology, Vol. 4, 1971, pp. 101-112.
8. Roberts, R., L. D. Aceto, R. Keilback, D. P. Teixeira, and J. M. Bonnell: An Analytical Model for Nitric Oxide Formation in a Gas Turbine Combustion Chamber. AIAA Paper No. 71-715, 1971.
9. Mosier, S. A., R. Roberts, and R. E. Henderson: Development and Verification of an Analytical Model for Predicting Emissions from Gas Turbine Engine Combustors During Low Power Operation. 41st Meeting Propulsion and Energetics Panel of AGARD, 1973.
10. Edelman, R. and C. Economos: A Mathematical Model for Jet Engine Combustor Pollutant Emissions. AIAA Paper No. 71-714, 1971.

The foregoing methods are lacking primarily in their ability to properly account for mixing phenomena occurring in the reverse flow recirculation zone of combustion devices. It has recently become feasible, however, to treat more rigorously flows having recirculation zones, by numerical solution of elliptic equations governing combusting flows. For example, one such numerical method based on an explicit point-by-point relaxation procedure has been suggested by Gosman, et al., (Ref. 11). Sample calculations of a representative gas turbine combustor flow have been computed at United Technologies Research Center using the Gosman, et al. method, to demonstrate the feasibility of making computations in the recirculating zones of combustion chambers. The results obtained with this procedure demonstrated qualitative agreement with experimental observations (Ref. 12).

Although these results were very encouraging, the slow convergence properties of the Gosman, et al. procedure, arising primarily from the use of a point-by-point relaxation technique, became apparent. Consequently, an improved numerical procedure was developed at UTRC for solving combusting flows containing recirculation zones. The UTRC procedure is an implicit computational scheme, and is novel in that residuals are relaxed simultaneously throughout the entire flow field, rather than one at a time, as is characteristic of the explicit point methods. Under a joint AFAPL/FAA contract, the UTRC Field Relaxation Elliptic Procedure (FREP) based on the rigorous solution of the governing equations was further developed and used to predict the performance and emission characteristics of can-annular and annular gas turbine combustors (Ref. 13). Further development of the procedure and the physical models is presently being carried out under EPA Contract No. 68-02-1873. The UTRC method solves the axisymmetric time-averaged Navier-Stokes equations including the effects of turbulence, chemistry, radiation, and droplet vaporization. The FREP code has given reasonable predictions for combustor flow fields which have axial symmetry; however, significant circumferential asymmetry is present in many aircraft combustor flow fields and a realistic approach must consider this complication. Such a general approach involves solution of the time averaged three-dimensional Navier-Stokes equations including turbulence, chemical reactions, radiation transport and droplet vaporization. Recently, for instance, Patankar and Spalding (Ref. 14) have developed

---

11. Gosman, A. D., W. M. Pun, A. K. Runchal, D. B. Spalding, and M. Wolfshtein: Heat and Mass Transfer in Recirculating Flows. Academic Press, New York, 1969.
12. Anasoulis, R. F.: Computations of the Flow in a Combustor. United Aircraft Research Laboratories Report K110885-1, November 1971.
13. Anasoulis, R. F., H. McDonald and R. C. Buggeln: Development of a Combustor Flow Analysis, Part I: Theoretical Studies. Air Force Aero Propulsion Laboratory Report AFAPL-TR-73-98, Part I, January 1974.
14. Patankar, S. V. and D. B. Spalding: A Computer Model for Three-Dimensional Flow in Furnaces, Fourteenth Symposium (International) on Combustion, The Combustion Institute, 1973, pp. 606-614.

a line relaxation procedure for computation of steady three-dimensional combusting flows in cartesian geometries; however, this procedure is not generally available and few details of this technique are known.

The objective of the present investigation was to extend an existing and relatively efficient UTRC three-dimensional Navier-Stokes calculation procedure (Ref. 15) so that it would be able to compute combusting flows. In particular, the procedure developed includes a simple mixing length turbulence model, a pseudo-kinetic hydrocarbon chemistry model, a liquid droplet vaporization model, a single frequency radiation model and a finite rate nitrogen oxide chemistry model. The intent in the development of the flow models described above was to eliminate undue complexity and sophistication, simultaneously providing a reasonably good framework within which refinements could be easily implemented at a future time, if warranted by comparisons with experimental data.

---

15. Briley, W. R. and H. McDonald: An Implicit Numerical Method for the Multidimensional Compressible Navier-Stokes Equations. United Aircraft Research Laboratories Report M911363-6, November 1973.

SECTION II

THEORETICAL ANALYSIS

Approach

The flow regime considered in the present study is a steady or unsteady gas-phase flow with hydrocarbon chemistry, droplet vaporization and burning, and radiation transport. An equilibrium mixing length model with a generalized eddy viscosity is used to specify the turbulent momentum fluxes (Reynolds' stress) in the time-averaged Navier-Stokes equations. The turbulent fluxes of enthalpy and chemical species are determined by specifying turbulent exchange coefficients using values for effective Prandtl and Schmidt numbers taken from knowledge of turbulent flow of gases and gas mixtures. In addition, a chemistry model, a droplet model, and a radiation model are necessary to include the effects of chemical reactions, two phase flow, and radiation emission and absorption on the combustor flow field.

A computational method is required to solve the complex system of equations obtained for combusting flows using the physical models described above. The computational procedure must be capable of treating the flow field resulting from the mixing and chemical reaction of the appropriate chemical species, and from large gradients in flow properties caused by the combustion process. The Multidimensional Implicit Nonlinear Time-dependent (MINT) technique developed by Briley and McDonald (Ref. 15) for the compressible Navier-Stokes equations is well suited for application to the complex equations governing combusting flows and was employed in the present study. The MINT procedure is particularly attractive in view of its economic computer storage requirements (only a portion of the flow is required in core at any given time) and its high efficiency relative to other available schemes. The resulting computer code is used to compute time-mean-average velocities, temperatures, pressures and species concentrations within a selected combustor with discrete inlet injection ports, and the results are compared with the available experimental measurements to allow an evaluation of the procedure and the analytical modeling techniques.

Governing Equations

Under consideration is the flow of a turbulent chemically reacting multicomponent mixture with heat and mass transport. The governing system of partial differential equations describing the combustion process is based on the

conservation laws of mass, momentum, energy, and chemical species (Ref. 16). For simplicity these equations are expressed in vector notation below and all quantities are nondimensional. Velocities are normalized by U_D, density by ρ_D, enthalpy by h_D, temperature by T_D, molecular weights by W_D, pressure by $p_D = \rho_D R_g T_D Z_D (Z_D = 10^3/W_D)$, dynamic viscosity by μ_D, radiation energy flux by q_{R_D}, and time by (L/U_D) where L is the reference length. Coupling between concentration and thermal gradients (Soret and Dufour effects), pressure gradient diffusion, body forces and bulk viscosity are all assumed to be negligible. In addition, Fick's law is presumed valid which implies equal binary diffusion coefficients for each pair of species in the mixture (see, e.g., Ref. 17). The resulting set of time-averaged equations is

Continuity

$$\frac{\partial \rho}{\partial t} = -\nabla \cdot (\rho \vec{u}) \tag{1}$$

Conservation of Gas Phase Species

$$\frac{\partial (\rho m_i)}{\partial t} = -\nabla \cdot (\rho \vec{u} m_i) + \frac{1}{Re} \nabla \cdot (\Gamma_m \nabla m_i) + r_i + \sum_j s_{i,j} \tag{2}$$

Conservation of Liquid Phase Species

$$\frac{\partial (\rho f_j)}{\partial t} = -\nabla \cdot (\rho \vec{u} f_j) + \frac{1}{Re} \nabla \cdot (\Gamma_p \nabla f_j) + R_j \tag{3}$$

Conservation of Momentum

$$\frac{\partial (\rho \vec{u})}{\partial t} = -\nabla \cdot (\rho \vec{u}\vec{u}) - \frac{p_D}{\rho_D U_D^2} \nabla_p + \frac{1}{Re} \nabla \cdot \left(2\mu_{eff} \bar{\bar{e}}\right) - \frac{2}{3} \frac{1}{Re} \nabla \left[\mu_{eff} (\nabla \cdot \vec{u})\right] \tag{4}$$

Conservation of Energy

$$\begin{aligned} \frac{\partial (\rho H)}{\partial t} = & -\nabla \cdot (\rho \vec{u} H) + \frac{p_D}{\rho_D h_D} \frac{\partial p}{\partial t} + \frac{1}{Re} \nabla \cdot (\Gamma_h \nabla H) \\ & + \frac{1}{Re} \frac{U_D^2}{h_D} \nabla \cdot \left[\left(\mu_{eff} - \Gamma_h\right) \nabla \left(\frac{\vec{u} \cdot \vec{u}}{2}\right)\right] \\ & + \frac{1}{Re} \nabla \cdot \left[\left(\Gamma_m - \Gamma_h\right) \sum_i h_i \nabla m_i\right] - \frac{1}{Bo} \nabla \cdot \vec{q}_R - \sum_i r_i h_i^f \end{aligned} \tag{5}$$

---

16. Bird, R. B., W. E. Stewart, and E. N. Lightfoot: Transport Phenomena. Wiley, New York, 1960.
17. Williams, F. A.: Combustion Theory. Addison-Wesley, Reading, Massachusetts, 1965.

The mean flow rate of strain tensor in Eq. (4) is given by

$$\bar{\bar{e}} = \frac{1}{2}\left[(\nabla\vec{u})+(\nabla\vec{u})^T\right] \tag{6}$$

The necessary thermodynamic relationships are

$$p = \rho T Z \tag{7a}$$

$$Z = \frac{1}{W_m} = \sum_i \frac{m_i}{W_i} \tag{7b}$$

$$H = \sum_i m_i h_i + \frac{1}{2}\frac{U_D^2}{h_D}(\vec{u}\cdot\vec{u}) \tag{8}$$

and the enthalpy of species i is

$$h_i = \int_{T_f}^{T} C_{p_i}(T)\, dT \tag{9}$$

Note that the heat of formation (h_i^f) of species i does not appear in the definition Eq. (9), but rather has been included explicitly in the energy conservation equation (5). This formulation was found beneficial in the present procedure in order to reduce numerical difficulties due to truncation errors. The kinetic heating terms in the energy equation which are not significant for the Mach numbers under consideration, have been neglected.

In order to solve the above system of equations, in addition to boundary conditions, it is necessary to specify the turbulent exchange coefficients μ_{eff}, Γ_h, Γ_m, Γ_p; the rate of production of species i due to chemical reactions r_i, the source due to vaporization of liquid droplets from particle class j, $s_{i,j}$; the droplet source term R_j^p; and the radiation energy source term, $-\nabla\cdot\vec{q}_R$. In the present analysis since effective Prandtl and Schmidt numbers are defined from knowledge of turbulent flows of gases and gas mixtures, only the turbulent momentum exchange coefficient, μ_{eff}, must be specified. The energy and species exchange coefficients are obtained from the relations

$$\Gamma_h = \frac{\mu_{eff}}{Pr_{eff}} \tag{10}$$

$$\Gamma_m = \Gamma_p = \frac{\mu_{eff}}{Sc_{eff}} \tag{11}$$

A turbulence model is employed to define the effective viscosity, μ_{eff}. Similarly, a chemistry model is employed to specify the production rate r_i for hydrocarbon and nitrogen oxide chemistry, a droplet vaporization model is employed for the source terms R_j and $s_{i,j}$, and a radiation transport model serves to specify $\nabla \cdot \vec{q}_R$. These models will be discussed in detail subsequently.

Geometry and Coordinate System

The governing vector equations presented above must be written in a coordinate system appropriate for combustor flow. In the present study consideration was directed primarily toward three-dimensional flows in axially symmetric combustor geometries with a discrete circumferential distribution of air and fuel injection ports. Rectangular duct geometries may also be treated quite easily within this framework. To obtain axisymmetric coordinates of sufficient generality, a two-dimensional orthogonal curvilinear coordinate system is rotated about an axis of symmetry to produce the desired geometry (Fig. 1). The axisymmetric coordinates are derived from a general system of orthogonal curvilinear coordinates x_1, x_2, x_3 with metric coefficient h_1, h_2, h_3. The vector operations necessary for deriving the governing differential equations in this coordinate system from the vector equations (1) through (5) may be found in Ref. 18. These are summarized in Appendix A for completeness. These vector relations may be substituted into equations (1) to (5) to obtain the governing equations in the generalized coordinate system. The system of axisymmetric coordinates are obtained by taking $h_2 = r$ and $x_2 = \theta$, where r is the radial distance from the axis of symmetry and θ is the angular coordinate (Fig. 1).

Turbulence Model

The flow in combustion devices is known to be predominantly turbulent. To account for this turbulent behavior in the solution of the time-averaged Navier-Stokes equations, a turbulence model is introduced to define an effective viscosity. A review of turbulence models is available in the literature (see, e.g., Refs. 19 and 20). Prandtl (Ref. 21) was perhaps the first to introduce a turbulence model when he postulated that the time-averaged shear

---

18. Emmons, H. W., ed.: Fundamentals of Gas Dynamics. High Speed Aerodynamics and Jet Propulsion, Vol. 3, Princeton University Press, Princeton, N. J., 1958.
19. Launder, B. E. and D. B. Spalding: Mathematical Models of Turbulence. Academic Press, London, 1972.
20. Harlow, F. H., ed.: Turbulence Transport Modeling. AIAA Selected Reprint Series, Vol. XIV, 1973.
21. Prandtl, L.: Bericht Uber Untersuchingen Zur Ausgebildeten Turbulenz. ZAMM, Vol. 5, 1925, p. 136.

stress and the time-averaged velocity gradient are proportional as in laminar flow, and that the length scale (the so-called mixing length) which enters the relationship is proportional to the turbulent shear region thickness. Prandtl's mixing length model has been employed successfully by a number of investigators (e.g., Refs. 22 to 26) in a variety of problems primarily involving turbulent flow along walls and in free turbulent flows. A disadvantage of the mixing length model is that is is an equilibrium model (i.e., turbulence is assumed to be produced and dissipated locally) and it requires an ad hoc mixing length distribution. Some of the shortcomings of the mixing length model have been overcome for many cases of interest by the introduction of various multiequation transport models of turbulence. A principal disadvantage of the multiequation turbulence models from a computational viewpoint is the necessity of solving additional transport equations. In view of the preliminary nature of the present work a mixing length model is employed for several reasons. First of all, an ad hoc mixing length can be assumed which does give a reasonable representation of the turbulent process, and thus is expected to give reasonable theoretical predictions. Secondly, it is a definite advantage to keep the physical models (turbulence, chemistry, droplet, radiation) relatively simple to allow verification of the basic three-dimensional numerical calculation procedure at this point in time.

The formulation of the mixing length turbulence model employed in this analysis is based on the mixing length distribution suggested by Williamson (Ref. 25) for flow in ducts and pipes. In mathematical terms the expression for the effective viscosity takes the form (Ref. 27)

$$\frac{\mu_{eff}}{Re} = \rho \ell^2 (2\bar{\bar{e}} : \bar{\bar{e}})^{1/2} \tag{12}$$

where the mixing length ℓ is given by

---

22. Patankar, S. V. and D. B. Spalding: Heat and Mass Transfer in Boundary Layers. Intertext Books, London, 1970.
23. Maise, G. and H. McDonald: Mixing Length and Kinematic Eddy Viscosity in a Compressible Boundary Layer. AIAA Journal, Vol. 6, 1968, pp. 73-80.
24. McDonald, H. and F. J. Camarata: An Extended Mixing Length Approach for Computing the Turbulent Boundary Layer Development. Proceedings of the AFOSR-IFP-Stanford Conference on Boundary Layer Prediction, 1968.
25. Williamson, J. W.: An Extension of Prandtl's Mixing Length Theory. Applied Mechanics and Fluids Engineering Conference, ASME, June 1969.
26. Lilley, D. G.: Prediction of Inert Turbulent Swirl Flows. AIAA Paper No. 72-699. AIAA 5th Fluid and Plasma Dynamics Conference, June 1972.
27. Beer, J. M. and N. A. Chigier: Combustion Aerodynamics. Wiley, New York, 1972.

$$\frac{\ell}{r_o} = 0.14\left(\frac{y}{r_o}\right) \exp\left(1 - \frac{y}{r_o}\right) \tag{13}$$

Here r_o is the distance from the wall to the centerline of the duct or pipe, and y is the distance from the point in question to the nearest wall.

Special consideration must be given to calculation of turbulent flow in the vicinity of walls in view of the large flow gradients which occur there. Since the expense of simply increasing the number of grid points near a wall may be considerable, an analytical wall function formulation has been employed in the present study. A set of three universal velocity profiles (Ref. 28) are employed in the wall region, corresponding to the laminar sublayer ($y^+ \leq 4$), a transition region ($4 < y^+ < 26$), and the logarithmic law-of-the-wall region ($y^+ \geq 26$):

$$u^+ = y^+ \qquad \text{for } y^+ \leq 4 \tag{14a}$$

$$u^+ = c_1 \ln(1+y^+) + c_2 + \left[(1 - c_1 - c_2\, a)y^+ - c_2\right] e^{-ay^+} \qquad \text{for } 4 < y^+ < 26 \tag{14b}$$

$$u^+ = c_1 \ln y^+ + c_2 \qquad \text{for } y^+ \geq 26 \tag{14c}$$

where

$$u^+ = \frac{\tilde{u}}{u^*} \tag{15}$$

$$y^+ = y\left(\frac{\rho Re}{\mu_{lam}}\right) u^* \tag{16}$$

and

$$u^* = \left(\frac{\tau_w}{\rho Re}\right)^{1/2} \tag{17}$$

---

28. Walz, A.: Boundary Layers of Flow and Temperature. The M.I.T. Press, Cambridge, Massachusetts, 1969.

In Eq. (15) $\tilde{u}$ denotes the total velocity component parallel to the wall, and u^* is the nondimensional friction velocity, Eq. (17). The finite difference form of the velocity gradient at the grid point adjacent to the wall point is specified consistent with the appropriate universal profile given above. In the present formulation the assumption of constant shear stress in the immediate vicinity of the wall is utilized. The specification of the velocity gradient at the grid point adjacent to the wall (where the velocity is known) is equivalent to imposing a "slip" velocity at the wall itself. Hence flow resolution in the region very near the wall is sacrificed to attain accuracy in the central region of the flow field where the combustion processes are concentrated. However, if accurate calculations in the wall region are required at a later date, refinements to the wall function approach may be implemented easily in the present computational procedure.

Chemistry Model

The method employed for introducing the effects of hydrocarbon chemistry into the calculation procedure is based on solution of the fuel conservation equation with a specified pseudo-kinetic chemical rate term. The pseudo-kinetic approach simplifies the computational problem of incorporating the hydrocarbon chemical energy release into the present procedure, since local chemical equilibrium is achieved by increasing the chemical rate constant as a function of time to a sufficiently large value. Furthermore, a real (global) hydrocarbon kinetic mechanism may be incorporated into the present framework in a conceptually straightforward manner. The kinetic nitric oxide (NO) chemistry model used herein assumes that NO is a trace species which has a negligible effect on mixture properties and the energy deposition in the flow field. Therefore, the NO species conservation equation may be solved separately after determination of a steady solution with hydrocarbon chemistry.

Nitric Oxide Chemistry Analysis

Solution of the species Eq. (2) to account for convection, diffusion, and production of nitric oxide (NO) requires an expression for the rate of creation of nitric oxide, r_{NO}, due to chemical reactions. To develop this expression knowledge of the reaction mechanism by which nitric oxide is formed is required. A generally accepted reaction mechanism for NO formation and decomposition in post flame gases is that proposed by Lavoie, et al. (Ref. 29). It consists of the following six reactions:

---

29. Lavoie, G. A., J. B. Heywood, and J. C. Keck: Experimental and Theoretical Study of Nitric Oxide Formation in Internal Combustion Engines. Combustion Science and Technology, Vol. 1, 1970, pp. 313-326.

$$N_2 + O \rightleftharpoons NO + N \tag{18}$$

$$N + O_2 \rightleftharpoons NO + O \tag{19}$$

$$N + OH \rightleftharpoons NO + H \tag{20}$$

$$H + N_2O \rightleftharpoons N_2 + OH \tag{21}$$

$$O + N_2O \rightleftharpoons N_2 + O_2 \tag{22}$$

$$O + N_2O \rightleftharpoons NO + NO \tag{23}$$

The first two reactions, Eqs. (18) and (19) form the Zeldovich mechanism (Ref. 30) which is considered to be the principal nitric oxide formation reaction mechanism. The two reactions together with the third reaction, Eq. (20) which assumes minor importance under fuel rich conditions, form the extended Zeldovich mechanism which is employed in the present study. At low temperatures, when nitric oxide concentrations are much greater than equilibrium values, the fourth, fifth and sixth reactions, Eqs. (21) trhough (23), involving N_2O as an intermediary, may become important; however, because overall reaction rates are so low, the net effect of these reactions is probably negligible. Therefore, these reactions have been neglected in the present study. The results of Bowman and Seery (Ref. 31), as well as other investigators (Ref. 32) in investigation of nitric oxide formation kinetics in combustion processes, lend support to this approach.

With the reaction mechanism for nitric oxide defined by the extended Zeldovich mechanism, Eqs. (18) through (20), it becomes possible to develop an expression for the rate term, r_{NO}, entering in the chemical species equation, Eq. (2). The mathematical development of the rate term is based on the "Law of Mass Action," which states that the rate of chemical reaction is proportional to the active masses of the reacting materials. Thus, referring to Eqs. (18) through (20), rate expressions for nitric oxide and nitrogen can be written

---

30. Zeldovich, Ya. B., P. Ya. Sadounikov, and D. A. Frank-Kamenetskll: Oxidation of Nitrogen in Combustion. Academy of Sciences of USSR, Institute of Chemical Physics, Moscow-Leningrad, 1947.
31. Bowman, C. T. and D. J. Seery: Investigation of NO Formation Kinetics in the Combustion Process: The Methane-Oxygen-Nitrogen Reaction. Emissions from Continuous Combustion Systems. Plenum Publishing Company, New York, 1972.
32. Caretto, L. S., L. H. Muzio, R. T. Sawyer, and E. S. Starkman: The Role of Kinetics in Engine Emission of Nitric Oxide. Combustion Science and Technology, Vol. 3, 1971.

$$\frac{dC_{NO}}{dt} = k_{1f} C_{N_2} C_O + k_{2f} C_N C_{O_2} + k_{3f} C_N C_{OH} - k_{1b} C_{NO} C_N - k_{2b} C_{NO} C_O - k_{3b} C_{NO} C_H \tag{24}$$

and

$$\frac{dC_N}{dt} = k_{1f} C_{N_2} C_O + k_{2b} C_{NO} C_O + k_{3b} C_{NO} C_H - k_{1b} C_{NO} C_N - k_{2f} C_N C_{O_2} - k_{3f} C_N C_{OH} \tag{25}$$

where C_i denotes the concentration of species i (moles per unit volume), and k_f and k_b are the forward and backward rate constants (volume/mole-sec), respectively, for reactions (18) to (20), (subscripts 1, 2, 3). Because the relaxation time for Eq. (25) is several orders of magnitude shorter than for Eq. (24), it is a good approximation to assume a steady concentration for C_N. Setting $dC_N/dt = 0$, Eq. (25) may be solved for C_N:

$$C_N = \frac{k_{1f} C_{N_2} C_O + k_{2b} C_{NO} C_O + k_{3b} C_{NO} C_H}{k_{1b} C_{NO} + k_{2f} C_{O_2} + k_{3f} C_{OH}} \tag{26}$$

This equation may be substituted into Eq. (24) to yield an expression for dC_{NO}/dt as a function of the concentrations of O_2, N_2, O, H, OH, and NO, and the rate constants which are functions only of temperature. The correct nondimensional expression for the rate term, r_{NO}, to be employed in Eq. (2) is

$$r_{NO} = \frac{L}{\rho_D U_D Z_D} \left(W_{NO} \frac{dC_{NO}}{dt} \right) \tag{27}$$

where r_{NO} is the mass rate of production of nitric oxide.

The rate constants governing the nitric oxide reaction scheme, Eqs. (18) through (20), and utilized in Eqs. (24) and (25), are of the modified Arrhenius form

$$k_j = A_j T^{N_j} \exp(-B_j/RT) \tag{28}$$

where data for the activation energies, B_j, the frequency factors, A_j, and exponent N_j, are taken from Refs. (33) and (34) and tabulated in Table I. The concentrations appearing in Eq. (24) are determined using the chemical equilibrium computational analysis of Brinkley (Refs. 35, 36), with the amounts of hydrocarbon fuel and oxygen available for reaction determined from the pseudo-kinetic chemistry calculation described below.

It should be noticed that time-mean concentrations and temperature are employed in Eqs. (24), (26) and (28), even though the effects of turbulent fluctuations in these quantities may lead to significant errors (Ref. 37) in the local rate of production of nitric oxide, Eq. (27). The implications of these effects are not well understood at the present time, and few theoretical modeling approaches to the problem are available (e.g., Ref. 38) while even fewer have been evaluated.

Pseudo-Kinetic Hydrocarbon-Air Chemistry Analysis

The pseudo-kinetic chemistry model provides a convenient means for introducing the effects of hydrocarbon combustion into the present time-dependent computational procedure. The basic chemistry model assumes that the

---

33. Baulch, D. L., D. D. Drysdale, D. G. Horne, and A. C. Lloyd: Critical Evaluation of Rate Data for Homogeneous Gas Phase Reactions of Interest in High-Temperature Systems. Report No. 4 Department of Physical Chemistry, Leeds University, United Kingdom, December 1969.
34. Campbell, I. M. and B. A. Thrush: Reactivity of Hydrogen to Atomic Nitrogen and Atomic Oxygen. Trans. Faraday Soc. 64, Part 5, 1968, pp. 1265-1274.
35. Brinkley, S. R.: Computational Methods in Combustion Calculations, Combustion Processes, Section C. High Speed Aerodynamics and Jet Propulsion, Vol. 2, B. Lewis, R. N. Peace, and H. S. Taylor, eds., Princeton University, Princeton, N. J., 1956.
36. Brinkley, S. R.: Calculations of the Thermodynamic Properties of Multi-Component Systems and Evaluation of Propellant Performance Parameters. Proceedings of the First Conference on Kinetics, Equilibrium and Performance of High Temperature Systems, A. S. Bahn and E. E. Zukoski, eds. The Combustion Institute, 1960, pp. 74-81.
37. Gouldin, F. C.: Role of Turbulent Fluctuations in NO Formations. Combustion Science and Technology, Vol. 9, 1974, pp. 17-23.
38. Libby, P. A.: On Turbulent Flows with Fast Chemical Reactions, Part I: The Closure Problem. Combustion Science and Technology, Vol. 6, 1972, pp. 23-28.

the combustion process energy release is adequately described by a single step reaction of the form

$$C_n H_m + \nu_2 O_2 \rightarrow P \tag{29}$$

In the reaction (29) the hydrocarbon fuel C_nH_m combines with O_2 to produce products of combustion P, with the nitrogen in air being treated as an inert species. The necessary species conservation equations are

$$\frac{\partial(\rho m_1)}{\partial t} = -\nabla\cdot(\rho\tilde{u}m_1) + \frac{1}{Re}\nabla\cdot(\Gamma_m\nabla m_1) + r_1 \tag{30}$$

$$\frac{\partial(\rho\Phi)}{\partial t} = -\nabla\cdot(\rho\tilde{u}\Phi) + \frac{1}{Re}\nabla\cdot(\Gamma_m\nabla\Phi) \tag{31}$$

where m_1 is the mass fraction of unburned fuel, and Φ is a mixture fraction defined as

$$\Phi = R_s m_1 - m_2 \tag{32}$$

Here m_2 is the mass fraction of oxidizer (O_2) and R_s is the stoichiometric ratio, i.e., the ratio of oxidizer mass to fuel mass for reaction (29):

$$R_s = \frac{\nu_2 W_{O_2}}{W_{fuel}} \tag{33}$$

where W_{O_2} and W_{fuel} are the molecular weights of oxidizer (O_2) and fuel (C_nH_m), respectively, and ν_2 is the number of moles of oxidizer in reaction (29).

It can be shown that the mass fraction of inert species (primarily N_2) is given by

$$m_N = \frac{1 - f_o}{f_o + R_s}(R_s - \Phi) \tag{34}$$

where f_o is the mass fraction of O_2 in the oxidizer (f_o = 0.2322 for air). The mass fraction of the products of combustion is then

$$m_p = 1 - m_1 - m_2 - m_N \tag{35}$$

For simplicity it has been assumed that the reaction (29) for methane proceeds stoichiometrically, so that ν_2=2 and the products of combustion are $P=CO_2+2H_2O$. This assumption adequately represents the energetics of methane-air combustion. In the present analysis the pseudo-chemical production rate r_1 in Eq. (30) is chosen to force the fuel mass fraction m_1 to its equilibrium value, m_{1e}.

$$r_1 = -k_{HC}\left(m_1 - m_{1e}\right) \tag{36}$$

The rate constant k_{HC} is increased as a function of time to a sufficiently large value to insure achievement of equilibrium. The justification for the chemical equilibrium approximation is based on the observation that, for many combustors, the temperature and pressure conditions are such that the fuel oxidation reactions go to completion rapidly. A nonequilibrium chemistry model could be implemented in the present procedure at a later time if it is warranted by comparison with experimental data.

For present purposes it is adequate to assume that at a given point either all the fuel or all the oxidizer is consumed in the equilibrium state. Hence, for combustion governed by reaction (29) the equilibrium fuel mass fraction is given by

$$\begin{aligned} m_{1e} &= \frac{1}{R_s}\,\Phi \qquad && \text{for } \Phi \geq 0 \\ m_{1e} &= 0 && \text{for } \Phi < 0 \end{aligned} \tag{37}$$

The energy deposition rate term, $\sum_i r_i h_i^f$, in the stagnation enthalpy equation (5) takes the following form for the combustion reaction (29):

$$\sum_i r_i h_i^f = r_1 \left[h_1^f - h_p^f + R_s \left(h_2^f - h_p^f \right) \right] \tag{38}$$

where h_1^f, h_2^f, and h_p^f are the heats of formation for the fuel, oxidizer and combustion products, respectively.

The species concentrations which are required for the NO chemistry, Eq. (24), are determined using a chemical equilibrium analysis (Ref. 35, 36). However, the present application may be considered as a "partial-equilibrium" analysis, since the amounts of hydrocarbon fuel and oxygen which have reacted are determined from the pseudo-kinetic model as follows. The solution to Eqs. (30) and (31) yields the mass fractions of (unburned) fuel and oxygen, m_1 and m_2, existing at a given point. It is easily shown that the total fuel and air mass fractions present in the absence of chemical reactions are given by

$$m_1^* = \frac{\Phi + f_o}{R_s + f_o} \tag{39}$$

and

$$m_{air}^* = 1 - m_1^* = \frac{-\Phi + R_s}{R_s + f_o} \tag{40}$$

so that the corresponding oxygen mass fraction is

$$m_2^* = f_o\, m_{air}^* \tag{41}$$

Finally, the mass fractions of fuel (m_{HC}) and oxygen (m_{O_2}) which have reacted are

$$m_{HC} = m_1^* - m_1 \tag{42}$$

$$m_{O_2} = m_2^* - m_2 \tag{43}$$

It is now assumed that the hydrocarbon and oxygen which disappeared kinetically reacted in an equilibrium manner. In the partial equilibrium calculation the contributions from the species not available for reaction, m_1 and m_2, are assumed to be inert within the equilibrium chemistry procedure. Their contribution to the equilibrium composition comes only from their contribution to the energy of the mixture. The use of the above formulation with the constraints of specified pressure and enthalpy permits the calculation of the species concentrations appearing in Eq. (24).

Droplet Model

The injection of liquid fuel into combustors by atomizers results in the formation of a spatial distribution of liquid droplets within a specified size range. The acceleration, evaporation, and eventual burning of these droplets are important considerations in the performance of combustors. Accordingly, a droplet model is employed in this study to account for the influence of droplets on combustor performance.

The combustion of droplet sprays is directly influenced by the droplet size range, generally between 75 and 125 microns for most practical liquid fuels. In addition to droplet size, droplet combustion rates are also affected by local mixture properties and the relative velocity between the droplet and surrounding gas. Due to the complexity, the effects of these parameters on droplet burning rates have only been investigated for single isolated droplets. Accordingly, the subsequent droplet model development is necessarily dependent to a certain extent on contributions from single droplet analyses.

The droplet model employed in this study accounts for convection, diffusion, evaporation and burning of liquid droplets. The model is based on

solution of the particle fraction equations (Refs. 39 and 40) having as dependent variable the particle fraction, f_j, which represents the mass fraction of liquid contained in an incremental droplet size range (see Fig. 2). The particle fraction equation (3) is again

$$\frac{\partial(\rho f_j)}{\partial t} = -\nabla\cdot(\rho\bar{u}f_j) + \frac{1}{Re}\nabla\cdot\left(\Gamma_p\nabla f_j\right) + R_j$$

where Γ_p is the liquid phase eddy diffusivity coefficient, and R_j represents the rate of production of particles in class j due to all sources. One particle fraction equation is needed for each particle class studied. Although in principle the method allows for an infinite number of particle classes, computer time and storage considerations have set a limit of four particle classes in the present analysis. Solution of the particle fraction equations is sufficient to define the distribution of droplet sizes existing at each location in the flow field.

Implicit in the use of the droplet model are certain underlying assumptions which are listed as follows:

(1) The droplets form a cloud of suspended particles.

(2) The volume of droplets is negligible compared to gas volume.

(3) Relative velocity of droplets and surrounding gas is negligible.

(4) Temperature and density of droplets is uniform.

(5) Gas and liquid phase transport coefficients are equal.

As a consequence of assumption (1) droplet-droplet interaction is neglected. Assumption (2) is merely a statement that droplet density is much greater than gaseous density, which simplifies the governing equations and associated computations. Assumptions (3) and (4) also lead to a simplification of the governing equations because under these conditions only terms describing

---

39. Gibson, M. M. and B. B. Morgan: Mathematical Model of Combustion of Solid Particles in a Turbulent Stream with Recirculation. Journal of the Institute of Fuel, December 1970.
40. Spalding, D. B.: Mathematical Models of Continuous Combustion. Emissions from Continuous Combustion Systems, Plenum Publishing Company, New York, 1972.

interphase mass transfer need be considered. Assumption (5) eliminates the need for defining liquid phase transport coefficients about which little is known. Justification for assumptions (3) through (5) come from the fact that droplet sizes in typical combustors can generally be expected to be small both in regard to physical size (low micron range) and with respect to the microscale of the turbulence. Under these conditions, the droplets respond closely to the mean and fluctuating components of the gaseous motion and can, therefore, be expected to exhibit similar transport behavior. (Droplet sizes large in comparison to the turbulence microscale do not follow the gas motion but behave as though suspended in a laminar flow field having the same mean motion as that of the turbulent flow.) Under these conditions there is not droplet diffusion. Solution of the particle fraction equation, Eq. (3), is straightforward in the computational procedure subject to appropriate expressions for the boundary conditions and the source term. The boundary conditions are readily formulated for a typical combustor (see section on Boundary Conditions). The source term in Eq. (3) is evaluated for particles in class (j) by assuming that mass gain is due to vaporization of particles originating in class (j+1) which thereby enter class (j). Mass loss for class (j) is due to vaporization of particles in class (j) which thereby enter class (j-1). That is, as indicated in Fig. 2, an increase in the number of particles within a given class is due only to the decrease in radii of particles which are initially in classes having larger radii. Under this study an increase in particle fraction due to condensation from the gaseous phase is excluded from consideration. By treating the loss or gain in particle fraction due to the change of radii from one particle class to another as a movement of particles whose radii are changing at a rate dr/dt, the rate of change of particle fraction, f_j, at the upper and lower radii boundaries can be formulated as follows:

$$\text{Rate of movement of particles from above } r_{j+1} \text{ to below } r_{j+1} = \frac{\rho f_{j+1}}{r_{j+2} - r_{j+1}} \left(\frac{dr}{dt}\right)_{j+1} \tag{44}$$

$$\text{Rate of movement of particles from above } r_j \text{ to below } r_j = \frac{\rho f_j}{r_{j+1} - r_j} \left(\frac{dr}{dt}\right)_j \tag{45}$$

In addition to the two terms represented by Eqs. (44) and (45), which represent mass transfer across adjacent particle class boundaries, the source term in the particle fraction equations must contain a third term which represents loss of mass directly to the gaseous phase. This term can be represented as

$$\text{Loss of mass to gaseous phase} = \int_{r_j}^{r_{j+1}} \frac{\rho f_j}{r_{j+1} - r_j} \frac{3}{r} \frac{dr}{dt}\, dr \tag{46}$$

Employing Eqs. (44) through (46), the complete expression for the source term for the j^{th} particle class becomes

$$R_j = -\frac{\rho f_{j+1}}{r_{j+2} - r_{j+1}} \left(\frac{dr}{dt}\right)_{j+1} + \frac{\rho f_j}{r_{j+1} - r_j} \left(\frac{dr}{dt}\right)_j + \int_{r_j}^{r_{j+1}} \frac{\rho f_j}{r_{j+1} - r_j} \frac{3}{r} \frac{dr}{dt}\, dr \tag{47}$$

Assuming that the droplets are spherical and of constant density, it can easily be shown that

$$\frac{dr}{dt} = -\frac{\dot{m}}{4\pi r^2 \rho_d} \leq 0 \tag{48}$$

where ρ_d is the droplet density and $\dot{m}$ represents the rate of mass loss of a particle due to vaporization. A semi-empirical expression for $\dot{m}$ used in this study has been derived from a single droplet analysis (Ref. 41 and 42), and has the form

$$\dot{m} = 4\pi r\, \bar{m}_d \tag{49}$$

and

$$\bar{m}_d = \frac{\mu_{eff}}{Pr_{eff}} \ln \left\{ 1 + h_v \left[c_p (T_g - T_b) + \frac{h_c m_{2g}}{s} \right] \right\} \tag{50}$$

where h_v is the heat of vaporization per unit mass for liquid fuel at the temperature T_g (the surrounding gas temperature), T_b is the liquid boiling temperature, h_c is the heat of combustion per unit mass of oxygen for the chemical reaction considered, s is ratio of oxygen mass to fuel mass for the reaction considered, and m_{2g} is the mass fraction of oxygen in the surrounding gas.

Using Eq. (49) in Eq. (48), one obtains

$$\frac{dr}{dt} = -\frac{\bar{m}_d}{\rho_d r} \tag{51}$$

---

41. Wise, H., J. Lorell, and B. J. Wood: The Effects of Chemical and Physical Parameters on the Burning Rate of a Liquid Droplet. Fifth Symposium (International) on Combustion, The Combustion Institute, 1955.
42. Wood, B. J., W. A. Rosser, and H. Wise: Combustion of Fuel Droplets. AIAA Journal, Vol. 1, No. 5, May 1973.

Substituting this expression into Eq. (47) and integrating the last term of that equation yields the final form for the droplet source term:

$$R_j^p = -\frac{\rho \bar{m}_d}{\rho_d} \left\{ \frac{f_j}{r_j} \left[\frac{1}{r_{j+1} - r_j} + \frac{3}{r_{j+1}} \right] - \frac{f_{j+1}}{r_{j+1}\left(r_{j+2} - r_{j+1}\right)} \right\} \tag{52}$$

Equation (52) represents the rate of fuel loss to the gaseous phase as a result of vaporization. It also includes the mass burning rate of the droplet because of the equilibrium assumption employed in the analysis wherein the chemical reaction is presumed to go to completion and to occur instantaneously.

Radiation Model

It is well known that gases and other substances at high temperatures emit energy in the form of electromagnetic radiation. The purpose of the radiation model employed under this investigation is to define the radiant energy contribution to combustion heat transfer rates. Specifically, this model is employed to define the radiant energy source term, $-\nabla \cdot \vec{q}_R$, entering the energy equation (5), through which coupling between the radiation, convection, and conduction modes of heat transfer occurs. Unless the gaseous medium in a combustion chamber is strongly absorbing, the effect of radiation will generally be to reduce the peak temperatures in the flow field while wall surface temperatures will increase due to the possibly large radiant heat flux reaching the surface. In these cases, accurate prediction of combustor performance and emission characteristics will require a reasonable representation of the radiative transfer process. The radiative energy transfer process is inherently different from conductive and convective heat transfer processes since, in the latter two cases, energy is transferred by molecular collision and transport, whereas radiative energy transfer does not require molecular contact. The emission and absorption of thermal radiation is due to transitions between the energy levels of the atoms or molecules of the gas, and transitions involving free electrons.

The preliminary radiation transport model employed in this study is a discrete-flux model (Ref. 43). Similar methods have been employed with some

---

43. Gosman, A. D. and F. C. Lockwood: Incorporation of a Flux Model for Radiation into a Finite-Difference Procedure for Furnace Calculations. Fourteenth Symposium (International) on Combustion, The Combustion Institute, 1973, pp. 661-671.

success by other investigators (e.g., Refs. 44 through 46), and they are described in the literature (Refs. 46 through 48). The procedure developed in Ref. 43 is an ad hoc extension of the one-dimensional transport models proposed by Schuster, Schwarzchild, and Hamaker (see Ref. 48 for other references), in which discrete radiation fluxes in each of the positive and negative coordinate directions are considered. In the present study the radiation field will be assumed to be nearly axisymmetric for axisymmetric combustor geometries so that only fluxes in the radial and axial directions need be considered (the four-flux model, Ref. 43). For rectangular geometries a six-flux model (Ref. 14) is easily implemented. Since the four-flux model has been described elsewhere (Refs. 43 and 49), only the six-flux model will be outlined here.

Consider forward and backward fluxes, q_i^+ and q_i^-, in the coordinate direction x_i. The governing equations for a grey emitting and absorbing medium in local thermodynamic equilibrium including isotropic scattering may be written in Cartesian coordinates (i = 1, 2, 3) as:

$$\frac{dq_i^+}{dx_i} = -(\alpha_a + \alpha_s) q_i^+ + \left(\frac{\sigma T_D^4}{q_{R_D}}\right) \alpha_a T^4 + \frac{\alpha_s}{6} \sum_{j=1}^{3} \left(q_j^+ + q_j^-\right) \tag{53}$$

$$-\frac{dq_i^-}{dx_i} = -(\alpha_a + \alpha_s) q_i^- + \left(\frac{\sigma T_D^4}{q_{R_D}}\right) \alpha_a T^4 + \frac{\alpha_s}{6} \sum_{j=1}^{3} \left(q_j^+ + q_j^-\right) \tag{54}$$

where α_a and α_s are the so-called "flux" absorption and scattering coefficients (Ref. 43), σ is the Stefan-Boltzmann constant, and T is the absolute temperature. Before solution of the transport equations (53) and (54) can be

---

44. Chen, J. C.: Simultaneous Radiative and Convective Heat Transfer in an Absorbing, Emitting and Scattering Medium in Slug Flow Between Parallel Plates. AIChE Journal, Vol. 10, No. 2, March 1964.
45. Larkin, B. K. and S. W. Churchill: Heat Transfer by Radiation Through Porous Insulations. AIChE Journal, Vol. 5, No. 4, December 1959.
46. Hottel, H. C. and A. F. Sarofim: Radiative Transfer. McGraw-Hill, New York, 1967.
47. Zeldovich, Ya. B. and Yu. P. Raizer: Physics of Shock Waves and High-Temperature Hydrodynamic Phenomena. Vols. I and II, Academic Press, New York, 1966.
48. Siddall, R. G.: Flux Methods for the Analysis of Radiant Heat Transfer. Journal of the Institute of Fuel, June 1974, pp. 101-109.
49. Anasoulis, R. F. and H. McDonald: A Study of Combustor Flow Computations and Comparison with Experiment, EPA Report No. 650/2-73-045, December 1973.

attempted the mean absorption coefficient α_a and scattering coefficient α_s must be specified. Because scattering is generally of secondary importance in a particle-free gaseous medium of the type under consideration in the present study, the scattering coefficients will not be defined in this analysis. For an evaluation of the absorption coefficients, reliance is placed on the data available on emissivity of gases and gas mixtures (Refs. 50 to 52). The true absorption coefficients for air, water vapor, and carbon dioxide have been presented by Cess (Ref. 53) using the emissivity data available from the literature. For the present purposes it will be assumed that the necessary (frequency averaged) absorption coefficients are known functions of the thermodynamic state (e.g., pressure and temperature), and will not be considered further.

A considerable simplification of the transport equations (53) and (54) may be realized by writing them as a system of second-order equations, so that only three additional equations must be solved rather than six. For this purpose the following definitions are needed:

$$G_i = \frac{1}{2}\left(q_i^+ + q_i^-\right) \tag{55}$$

$$Q_i = q_i^+ - q_i^- \tag{56}$$

Manipulating Eqs. (53) and (54) with Eqs. (55) and (56) yields (with the scattering coefficient α_s retained for generality):

$$Q_i = -\frac{2}{\alpha_a + \alpha_s}\frac{dG_i}{dx_i} \tag{57}$$

and

$$\frac{dQ_i}{dx_i} = -2(\alpha_a + \alpha_s)G_i + \left(\frac{\sigma T_D^4}{q_{R_D}}\right)2\alpha_a T^4 + \frac{2}{3}\alpha_s\left(G_1 + G_2 + G_3\right) \tag{58}$$

---

50. McAdams, W. H.: Heat Transmission. McGraw-Hill, New York, 1954.
51. Hadvig, Sven: Gas Emissivity and Absorptivity: A Thermodynamic Study, Journal of the Institute of Fuel, Vol. 43, April 1970, pp. 129-135.
52. Taylor, P. B. and P. J. Foster: The Total Emissivities of Luminous and Nonluminous Flames. International Journal of Heat and Mass Transfer, Vol. 17, 1974, pp. 1591-1605.
53. Cess, R. D.: The Interaction of Thermal Radiation with Conduction and Convection Heat Transfer. Advances in Heat Transfer, Vol, 1, Academic Press, New York, 1964.

Finally, the combination of Eqs. (57) and (58) gives the desired result:

$$\frac{d}{dx_i}\left[\frac{1}{\alpha_a+\alpha_s}\frac{dG_i}{dx_i}\right] = \alpha_a\left[G_i - \left(\frac{\sigma T_D^4}{q_{R_D}}\right)T^4\right] + \alpha_s G_i - \frac{1}{3}\alpha_s\left(G_1+G_2+G_3\right) \tag{59}$$

The net rate of energy addition per unit volume due to thermal radiation is given by $-\nabla\cdot\vec{q}_R$. Since the components of $\vec{q}_R$ are simply the Q_i, Eq. (56), there follows

$$-\nabla\cdot\vec{q}_R = -\sum_{j=1}^{3}\frac{\partial Q_j}{\partial x_j} \tag{60}$$

and using Eq.(58) yields

$$-\nabla\cdot\vec{q}_R = -2\alpha_a\left[\left(\frac{\sigma T_D^4}{q_{R_D}}\right)3T^4 - \left(G_1+G_2+G_3\right)\right] \tag{61}$$

Therefore, solution of equation (59) for i = 1, 2, 3 provides the information necessary to determine $\nabla\cdot\vec{q}_R$ directly. Furthermore, the actual radiation energy fluxes, Q_i, may then be calculated using Eq. (57).

It is informative to consider the well-known limiting cases (see e.g., Ref. 54) of emission dominated radiative transfer ("optically thin" gas) and of near-radiative equilibrium ("optically thick"). In a nonscattering medium the frequency dependent optical depth is given by

$$\tau_\nu(\eta_s) = \int_0^{\eta_s}\alpha'_\nu(\eta)d\eta \tag{62}$$

where α'_ν is the true frequency dependent absorption coefficient and η is the path length. In the emission dominated limit $\tau_\nu \ll 1$, and in the present approximation one obtains for Eq. (61)

$$\nabla\cdot\vec{q}_R = 6\alpha_a T^4\left(\frac{\sigma T_D^4}{q_{R_D}}\right) \tag{63}$$

---

54. Vincenti, W. G. and C. H. Kruger, Jr.: Introduction to Physical Gas Dynamics. Wiley, New York, 1965.

The actual emission dominated result is from Ref. (54)

$$\nabla \cdot q_R = 4 \alpha_p T^4 \left(\frac{\sigma T_D^4}{q_{R_D}} \right) \tag{64}$$

where α_p is the Planck mean absorption coefficient. Therefore, the six-flux model will give the same result if $\alpha_a = 2/3\alpha_p$. In the optically thick limit ($\tau_\nu \gg 1$), the present model yields

$$G_i = T^4 \left(\frac{\sigma T_D^4}{q_{R_D}} \right) \tag{65}$$

so that,

$$Q_i = -\left(\frac{\sigma T_D^4}{q_{R_D}} \right) \frac{8}{\alpha_a} T^3 \frac{\partial T}{\partial x_i} \tag{66}$$

The correct thick gas equation is

$$Q_i = -\left(\frac{\sigma T_D^4}{q_{R_D}} \right) \frac{16}{3\alpha_R} T^3 \frac{\partial T}{\partial x_i} \tag{67}$$

where α_R is the Rosseland mean absorption coefficient (Ref. 54). These results are equivalent if $\alpha_a = 3/2\alpha_R$. A principal disadvantage of the discrete-flux model is the uncertainty in the value of the flux absorption coefficient α_a, which must actually depend on the local angular distribution of radiant intensity. Many of the approximate methods for treatment of radiation transport suffer from this problem; however, in recent years procedures have been developed for overcoming this difficulty (e.g., Ref. 55), but most are more troublesome to incorporate in the present time-dependent calculation procedure and may require considerably more computer time than a discrete-flux model. The ambiguity in the absorption coefficient appears greater with the six-flux model in view of the difference in coefficients of α_p and α_R obtained in the above limiting cases (i.e., $\alpha_a = 2/3\alpha_p$ for $\tau_\nu \ll 1$ and $\alpha_a = 3/2\alpha_R$ for $\tau_\nu \gg 1$). Comparison of Eqs. (53) and (54) with the corresponding

---

55. Traugott, S. C.: An Improved Differential Approximation for Radiative Transfer with Spherical Symmetry. AIAA Journal, Vol. 7, No. 10, Oct. 1969.

results of both the Schuster-Schwarzchild approximation (isotropic angular distribution of intensity) and the Schuster-Hamaker approximation (unidirectional radiation) reveals that the flux absorption coefficient (α_a) should equal $2\alpha_a'$ and α_a' in these two cases, respectively (where α_a' is the true absorption coefficient). Since information regarding the angular distribution of intensity is not known, it is necessary to consider the sensitivity of the predictions using this model both when performing calculations and when assessing the accuracy of the model.

Boundary Conditions

Solution of the governing partial differential equations requires specification of boundary conditions for each of the equations on all boundaries of the computational region. At a solid wall the density is determined implicitly using a three-point one-sided difference approximation of the continuity equation. The tangential velocities at a wall are determined implicitly through the use of the wall function approximation. The boundary conditions for each equation are given below in terms of the normal and tangential coordinates (n, s_1, s_2) at each surface. The radiation boundary conditions are considered separately at the end of this section.

Injection Ports:

u_n = specified

$u_{s_1} = u_{s_2} = 0$ or specified

ρ = specified

$\frac{\partial^2 p}{\partial n^2} = 0$

m_l = specified

ϕ = specified

f_j = specified

$m_{NO} = 0$

Solid Walls:

$u_n = 0$

u_{s_1}, u_{s_2} - wall function

ρ - continuity equation

$$\frac{\partial H}{\partial n} = \frac{\partial m_1}{\partial n} = \frac{\partial \Phi}{\partial n} = \frac{\partial f_j}{\partial n} = \frac{\partial m_{NO}}{\partial n} = 0$$

Axis or Plane of Symmetry:

$$\left.\begin{aligned} v &= 0 \\ \frac{\partial w}{\partial n} &= 0 \end{aligned}\right\} \quad \text{axis}$$

$$\left.\begin{aligned} \frac{\partial u_{s_1}}{\partial n} &= 0 \\ \frac{\partial u_{s_2}}{\partial n} &= 0 \end{aligned}\right\} \quad \text{plane}$$

$$u_n = 0$$

$$\frac{\partial \rho}{\partial n} = \frac{\partial H}{\partial n} = \frac{\partial m_1}{\partial n} = \frac{\partial \Phi}{\partial n} = \frac{\partial f_j}{\partial n} = \frac{\partial m_{NO}}{\partial n} = 0$$

Exit Plane:

$$p_{exit} = \text{specified}$$

$$\frac{\partial^2 u_n}{\partial n^2} = \frac{\partial^2 u_{s1}}{\partial n^2} = \frac{\partial^2 u_{s2}}{\partial n^2} = 0$$

$$\frac{\partial^2 H}{\partial n^2} = \frac{\partial^2 m_1}{\partial n^2} = \frac{\partial^2 \Phi}{\partial n^2} = \frac{\partial^2 f_j}{\partial n^2} = \frac{\partial^2 m_{NO}}{\partial n^2} = 0$$

The exit plane boundary conditions attempt to simulate the nearly unidirectional nature of the flow presumed to occur there.

The radiation boundary conditions in terms of the functions G_i remain to be defined.

(a) Opaque Wall of Prescribed Temperature

In this case the radiation flux at the surface is due only to reflection and emission, so that the desired boundary condition is

$$q_n^+ = \left(1-\epsilon_w\right) q_n^- + \epsilon_w T_w^4 \left(\frac{\sigma T_D^4}{q_{R_D}}\right) \tag{68}$$

where q_n^+ and q_n^- are the normal radiation flux components directed away from and toward the wall, respectively. Using Eqs. (55) through (57) in Eq. (68), yields

$$\frac{dG_i}{dn} = (\alpha_a + \alpha_s) \frac{\epsilon_w}{2-\epsilon_w} \left[G_i - T_w^4 \left(\frac{\sigma T_D^4}{q_{R_D}}\right)\right] \tag{69}$$

where n is the normal coordinate directed away from the surface in question.

(b) Outgoing Radiation Escapes

In this case there is no emission or reflection so that the incoming radiation must be specified,

$$q_n^+ = q_{in} \tag{70}$$

and one obtains

$$\frac{dG_i}{dn} = (\alpha_a + \alpha_s) \left[G_i - q_{in}\right] \tag{71}$$

(c) Axis or Plane of Symmetry

In this case the inward and outward fluxes are equal,

$$q_n^+ = q_n^- \tag{72}$$

and the desired condition is

$$\frac{dG_i}{dn} = 0 \tag{73}$$

SECTION III

COMPUTATIONAL ANALYSIS

Introduction

Exact analytical solutions of the time-averaged Navier-Stokes equations are rare due to their high order and coupled nonlinearity. As a result numerical methods must generally be employed for the solution of these equations. In addition, one of the major obstacles to the solution of the three-dimensional compressible Navier-Stokes equations is the large amount of computer time required, and consequently efficient computational methods are highly desirable. Most previous methods (for example, Refs. 56 to 59) have been based on explicit difference schemes for the unsteady form of the governing equations, and are subject to one or more stability restrictions on the size of the time step relative to the spatial mesh size. These stability limits usually correspond to the well-known Courant-Friedrichs-Lewy (CFL) condition and in some methods to an additional viscous stability condition. A key disadvantage of such conditionally stable methods is that the maximum time step is fixed by the spatial mesh size rather than the physical time dependence. If a steady solution is being computed as the asymptotic limit for large time of the unsteady solution as is the present objective, then using a small time step requires a large number of steps to reach the steady solution.

---

56. MacCormack, R. W.: Numerical Solution of the Interaction of a Shock Wave with a Laminar Boundary Layer. Proceedings of the Second International Conference on Numerical Methods in Fluid Dynamics; Springer-Verlag, New York, 1971, p. 151.
57. Allen, J. S. and S. I. Cheng: Numerical Solutions of the Compressible Navier-Stokes Equations for the Laminar Near Wake. Physics of Fluids, Vol. 13, No. 1, 1970, p. 37.
58. Roache, P. J. and T. J. Mueller: Numerical Solutions of Laminar Separated Flows. AIAA Journal, Vol. 8, No. 3, 1970, p. 530.
59. Victoria, K. J. and G. F. Widhopf: Numerical Solution of the Unsteady Navier-Stokes Equations in Curvilinear Coordinates: The Hypersonic Blunt Body Merged Layer Problem. Proceedings of the Third International Conference on Numerical Methods in Fluid Dynamics, Vol. II; Springer-Verlag, New York, 1973, p. 254.

In contrast to most explicit methods, many implicit methods tend to be stable for large time steps, and hence, offer the prospect of substantial increases in computational efficiency, provided of course that the computational effort per time step is competitive with that of the conditionally stable methods. An implicit method based on an alternating-direction-implicit (ADI) scheme has been developed at UTRC by Briley and McDonald (Ref. 15) for solution of the three-dimensional, compressible Navier-Stokes equations. This method will subsequently be referred to as the MINT (i.e., Multidimensional Implicit Nonlinear Time-Dependent) procedure. The MINT computer program has provided the basic numerical framework for development of the present combustor flow analysis. The MINT method has been described in detail in Ref. 15, but it will be summarized here for completeness. The method can be outlined briefly as follows: The governing equations are replaced by an implicit time difference approximation. Terms involving nonlinearities at the implicit time level are linearized by Taylor expansion about the solution at the known time level, and spatial difference approximations are introduced. The result is a system of multidimensional coupled (linear) difference equations for the dependent variables at the implicit time level. To solve these difference equations, the Douglas-Gunn (Ref. 60) procedure for generating alternating-direction-implicit (ADI) schemes as perturbations of fundamental implicit difference schemes is introduced. This technique leads to systems of one-dimensional coupled linear difference equations which can be solved efficiently by standard block-elimination methods. No iteration is required to compute the solution for a single time step, and for a k-point one-dimensional difference operator only 2k-1 arrays of information need be in core at any one time. The scheme is therefore very economical in terms of computer memory requirements.

Difference Notation

The governing equations (1-5) have three characteristics which are given special consideration in the numerical formulation; the equations are (1) nonlinear, (2) coupled, and (3) multidimensional. Before proceeding, some difference notation is introduced. The flow region is discretized by grid points having equal spacings, Δx_1, Δx_2, and Δx_3 in the x_1, x_2 and x_3 directions, respectively, and an arbitrary time step, Δt. Provisions for nonuniform grid spacing will be introduced subsequently. The subscripts i, j, k and superscript n are grid point indices associated with x_1, x_2, and x_3, and

---

60. Douglas, J. and J. E. Gunn: A General Formulation of Alternating Direction Methods. Numerische Math., Vol. 6, 1964, p. 428.

t, respectively. Thus, $\phi^n_{i,j,k}$ denotes $\phi\,(x_{1_i}, x_{2_j}, x_{3_k}, t^n)$ where ϕ can represent any of the dependent variables. The subscripts are frequently omitted if clarity is preserved, so that ϕ^n is equivalent to $\phi^n_{i,j,k}$. For convenience, the following shorthand difference-operator notation is used for derivative difference formulas:

$$\delta_1 \phi^n = \frac{-\phi^n_{i-1,j,k} + \phi^n_{i+1,j,k}}{2\Delta x_1} = \left.\frac{\partial \phi}{\partial x_1}\right|^n_{i,j,k} + O\left(\Delta x_1\right)^2 \tag{74}$$

$$\delta_1^2 \phi^n = \frac{\phi^n_{i-1,j,k} - 2\phi^n_{i,j,k} + \phi^n_{i+1,j,k}}{(\Delta x_1)^2} = \left.\frac{\partial^2 \phi}{\partial x_1^2}\right|^n_{i,j,k} + O(\Delta x_1)^2 \tag{75}$$

with analogous definitions for δ_2, δ_2^2, δ_3 and δ_3^2. It is assumed that the solution is known at the n level, t^n, and is desired at the (n+1) level, t^{n+1}.

Linearization Technique

The large time-step capabilities of implicit methods can place great demands on the linearization technique employed. Indeed, the favorable stability properties of implicit methods can be severely compromised by an inadequate linearization. The present technique, which can be used only in conjunction with an implicit difference scheme, permits the implicit solution of coupled nonlinear equations in one space dimension by a one-step noniterative scheme. This feature is retained for multidimensional problems by using ADI techniques. The linearization is accurate when variables change by relatively small amounts during a time step, and consequently, the accuracy of the linearization can be controlled by varying the time step. The linearization technique is also convenient for the implicit treatment of coupled nonlinear boundary conditions, and this latter feature has been found to have a highly favorable effect on the stability of the overall method (Ref. 15).

A technique is described for deriving linear implicit difference approximations for nonlinear differential equations. The technique is presented with reference to the following first-order equation in one dependent variable, $\phi\,(x, t)$:

$$\frac{\partial \phi}{\partial t} = F(\phi)\,\frac{\partial}{\partial x}\,G(\phi) \tag{76}$$

The procedure used here is based on an expansion of nonlinear implicit terms about the known time level, t^n, and leads to a one-step, two-level scheme which, being linear in unknown (implicit) quantities, can be solved efficiently without iteration. The technique is easily extended to treat coupled systems of equations and second-order spatial derivatives. The difference approximation is derived from the following backward time-difference replacement of Eq. (76):

$$\frac{\phi_i^{n+1} - \phi_i^n}{\Delta t} = \left[F(\phi)\,\frac{\partial}{\partial x}\,G(\phi)\right]_i^{n+1} + O(\Delta t) \tag{77}$$

where the spatial differencing of the bracketed term is as yet unspecified. Making use of chain-rule differentiation, the bracketed term in Eq. (77) is expanded about t^n; the result is then differenced using forward time differences and centered spatial differences to obtain the following implicit difference scheme:

$$\frac{\phi_i^{n+1} - \phi_i^n}{\Delta t} = F\left(\phi_i^n\right)\delta_x\,G\left(\phi_i^n\right) + \left\{F\left(\phi_i^n\right)\delta_x\left[\left(\frac{\partial G}{\partial \phi}\right)_i^n\left(\frac{\phi_i^{n+1}-\phi_i^n}{\Delta t}\right)\right] + \left(\frac{\partial F}{\partial \phi}\right)_i^n\left(\frac{\phi_i^{n+1}-\phi_i^n}{\Delta t}\right)\delta_x\,G\left(\phi_i^n\right)\right\}\Delta t \tag{78}$$

On examination, it can be seen that Eq. (78) is linear in ϕ^{n+1} and that all other quantities are either known or evaluated at the n level. Because of the spatial difference operator, δ_x, Eq. (78) contains ϕ_{i-1}^{n+1}, ϕ_i^{n+1}, and ϕ_{i+1}^{n+1}; consequently, the system of linear equations generated by writing Eq. (78) at each of the grid points, x_i, must be solved simultaneously as an implicit system. The implicit system of equations can be written in tridiagonal matrix form, and can therefore be solved easily and efficiently by standard techniques for tridiagonal systems (see, e.g., Ref. 61). The tridiagonal matrix structure emerges from writing Eq. (78) in the following form:

$$a_i^n\,\phi_{i-1}^{n+1} + b_i^n\,\phi_i^{n+1} + c_i^n\,\phi_{i+1}^{n+1} = d_i^n \tag{79}$$

---

61. Isaacson, E. and H. B. Keller: Analysis of Numerical Methods. Wiley, New York, 1966.

where the coefficients contain only n-level quantities. When applied at successive grid points, Eq. (79) generates a tridiagonal system of equations for ρ^{n+1}.

The linearization technique will be applied to the coupled Navier-Stokes equations in the following section, but first some general observations seem appropriate. The difference scheme has first-order accuracy in time, having been constructed from the backward difference replacement, Eq. (77). The formal temporal accuracy can be increased either by using a Crank-Nicolson centering about $t^{n+1/2}$ (i.e., by averaging the bracketed term in Eq. (77) between the n and (n+1) levels) or by using additional time levels in the difference replacement of time derivatives. However, temporal accuracy is not considered important for computing steady solutions using a time-dependent method; therefore, the fully-implicit backward difference formulation is considered adequate. It is also noted that if the original governing equation (76) has conservation form (F=1), then the linearization process preserves the conservation form for steady solutions.

Application of the Method

The extension of the numerical method to three dimensions is based on an alternating-direction implicit (ADI) technique. The original ADI method was introduced by Peaceman and Rachford (Ref. 62) and Douglas (Ref. 63); however, the alternating-direction concept has since been expanded and generalized. A discussion of various alternating-direction techniques is given by Mitchell (Ref. 64) and Yanenko (Ref. 65). Although much of the attention devoted to ADI methods has focused on single linear equations, a method for nonlinear hyperbolic systems of equations in two dimensions has been suggested by Gourlay and Morris (Ref. 66). Their method is a two-step procedure consisting of an explicit predictor step followed by an ADI corrector step.

---

62. Peaceman, D. W. and H. H. Rachford: The Numerical Solution of Parabolic and Elliptic Differential Equations. J. Soc. Indust. Appl. Math., Vol. 3, 1955, p. 28.
63. Douglas, J.: On the Numerical Integration of $u_{xx} + u_{yy} = u_t$ by Implicit Methods. J. Soc. Indust. Appl. Math., Vol. 3, 1955, p. 42.
64. Mitchell, A. R.: Computational Methods in Partial Differential Equations. Wiley, New York, 1969.
65. Yanenko, N. N.: The Method of Fractional Steps. Translation edited by M. Holt. Springer-Verlag, New York, 1971.
66. Gourlay, A. R. and J. Ll. Morris: Finite-Difference Methods for Nonlinear Hyperbolic Systems. Math. Comp., Vol. 22, 1968, p. 28.

The present technique is an application of the very general procedure developed by Douglas and Gunn (Ref. 60) for generating ADI schemes as perturbations of fundamental implicit difference schemes such as the backward-difference or Crank-Nicolson schemes. As with all ADI schemes, Douglas-Gunn schemes compute the solution for a time step in a sequence of intermediate steps, each of which usually involves treating derivatives implicitly in one of the coordinate directions. Although the solution of multidimensional implicit difference equations is normally time consuming, the one-dimensional difference equations appearing in these intermediate steps can be solved efficiently, and this is the attraction of ADI methods in general over other implicit methods. A less obvious feature of schemes generated by the Douglas-Gunn procedure is that, since they give the solution to a fundamental implicit difference scheme except for a small perturbation error, they can be viewed as an approximate technique for solving the fundamental difference scheme, rather than as difference schemes themselves. This unconventional view of the Douglas-Gunn procedure provides guidance in formulating the present method by indicating that the governing equations can be linearized and differenced in accordance with the backward difference scheme (or another implicit scheme) before the alternating-direction aspects of the method are introduced. Douglas-Gunn schemes also appear to have an advantage over locally one-dimensional (LOD) or "splitting" schemes, whose intermediate steps do not satisfy the consistency condition. The lack of consistency in the intermediate steps can present difficulties in the treatment of some boundary conditions and, according to Yanenko (Ref. 65, p. 33) does not permit the use of asymptotically large time steps.

The numerical method is essentially an application of the linearization technique of the previous section to the coupled system of governing equations (1-5). These equations are written in backward time difference form, and nonlinear implicit terms are linearized by expansion about t^n. The viscous force terms in Eq. (4) which contain mixed derivatives (i.e., $\partial^2 / \partial_{x_i} \partial_{x_j}$ for $i \neq j$) are most easily treated explicitly by evaluation at time level n. Although mixed derivatives can be differenced implicitly within the Douglas-Gunn framework, this would increase the number of intermediate steps and thereby complicate the solution procedure. For the solutions presented here and test cases computed by Briley and McDonald (Ref. 15), the explicit treatment of the aforementioned viscous terms had no observable adverse affect on stability. In three dimensions, optional artificial viscosity terms having the form $(\epsilon_1^n \delta_1^2 + \epsilon_2^n \delta_2^2 + \epsilon_3^n \delta_3^2)\, \phi^{n+1}$ are added to the difference equations, where ϕ represents ρ, u, v, w, H, m_1, Φ, f_j, and m_{NO}, respectively, in the continuity, x_1-, x_2-, x_3- momentum, energy, fuel species, hybrid species, particle fraction, and NO species equations. The difference equations obtained by the procedure just outlined represent a linearized backward difference

scheme. The equations can be arranged according to time and space derivatives, and written in the following matrix operator form (Ref. 15):

$$\bar{\bar{A}}^n \left(\frac{\bar{\phi}^{n+1} - \bar{\phi}^n}{\Delta t} \right) = \bar{\bar{D}}_1^n \bar{\phi}^{n+1} + \bar{\bar{D}}_2^n \bar{\phi}^{n+1} + \bar{\bar{D}}_3^n \bar{\phi}^{n+1} + \bar{S}^n \tag{80}$$

Here $\bar{\bar{A}}^n$ is a (mxm) matrix containing the time derivative coefficients, where m is the number of equations being solved; $\bar{\phi}$ is the column vector of the dependent variables; $\bar{\bar{D}}_1^n$, $\bar{\bar{D}}_2^n$, and $\bar{\bar{D}}_3^n$ are (mxm) matrices containing three-point difference operators associated with the coordinate directions x_1, x_2, and x_3, respectively; and $\bar{S}^n$ is a column vector containing only n-level terms.

Since the multidimensional implicit system with coefficients generated by Eq. (80) is difficult to solve, the Douglas-Gunn (Ref. 60) technique is applied to Eq. (80) to generate an ADI scheme. With the observation that the Douglas-Gunn procedure is being applied to a coupled system of equations, the following three-step scheme is obtained.

$$\bar{\bar{A}}^n \left(\frac{\bar{\phi}^* - \bar{\phi}^n}{\Delta t} \right) = \bar{\bar{D}}_1^n \bar{\phi}^* + \bar{\bar{D}}_2^n \phi^n + \bar{\bar{D}}_3^n \bar{\phi}^n + \bar{S}^n \tag{81}$$

$$\bar{\bar{A}}^n \left(\frac{\bar{\phi}^{**} - \bar{\phi}^n}{\Delta t} \right) = \bar{\bar{D}}_1^n \bar{\phi}^* + \bar{\bar{D}}_2^n \bar{\phi}^{**} + \bar{\bar{D}}_3 \bar{\phi}^n + \bar{S}^n \tag{82}$$

$$\bar{\bar{A}}^n \left(\frac{\bar{\phi}^{***} - \bar{\phi}^n}{\Delta t} \right) = \bar{\bar{D}}_1^n \bar{\phi}^* + \bar{\bar{D}}_2^n \bar{\phi}^{**} + \bar{\bar{D}}_3^n \bar{\phi}^{***} + \bar{S}^n \tag{83}$$

where $\bar{\phi}^*$, $\bar{\phi}^{**}$, and $\bar{\phi}^{***}$ are the intermediate solutions. Note that at each step of the scheme, one more coordinate direction is treated implicitly, and that the most recent approximation to $\bar{\phi}$ is not always used, as this would adversely affect the stability. Douglas and Gunn were able to show under fairly general assumptions that the ADI scheme, Eqs. (81-83), satisfies the consistency condition provided that the original difference scheme, Eq. (80), is consistent. Under more restrictive assumptions, they were able to show that the stability of the ADI scheme follows from that of the original difference scheme, and also that the final solution $\bar{\phi}^{***}$ approximates $\bar{\phi}^{n+1}$ with an error no worse than $O(\Delta t)^2$, and consequently, $\bar{\phi}^{***}$ can be accepted as $\bar{\phi}^{n+1}$. Although these results are not of sufficient generality to encompass the Navier-Stokes equations, it is often suggested (e.g., Ref. 67, p. 215)

---

67. Richtmyer, R. D. and K. W. Morton: Difference Methods for Initial Value Problems. Second Edition. Interscience, New York, 1967.

that the scheme is stable and accurate under conditions more general than those for which rigorous proofs are available. Consequently, the notion that the procedure as outlined here is applicable to the Navier-Stokes equations is adopted as a working hypothesis. Support for this hypothesis is provided by the favorable results obtained in actual computations (see Ref. 15).

The effort involved in the actual programming and solution of Eqs. (81-83) is greatly reduced, and the computer storage requirements are halved by subtracting Eq. (81) from Eq. (82) and Eq. (82) from Eq. (83), so that Eqs. (82-83) have the following simplified form:

$$\bar{\bar{A}}^n \left(\frac{\bar{\phi}^{**} - \bar{\phi}^{*}}{\Delta t} \right) = \bar{\bar{D}}_2^n \left(\bar{\phi}^{**} - \bar{\phi}^n \right) \tag{84}$$

$$\bar{\bar{A}}^n \left(\frac{\bar{\phi}^{***} - \bar{\phi}^{**}}{\Delta t} \right) = \bar{\bar{D}}_3^n \left(\bar{\phi}^{***} - \bar{\phi}^n \right) \tag{85}$$

Equations (84-85) in effect provide corrections to the previous intermediate solutions, $\bar{\phi}^*$ and $\bar{\phi}^{**}$, respectively, and serve to stabilize Eq. (81), which establishes consistency with the governing equations. For this reason, Yanenko (Ref. 65) has termed the Douglas-Gunn procedure the method of stabilizing corrections.

On examination, it can be seen that the difference equations (81, 84, 85) are linear in the *-level quantities. At the k^{th} step in the procedure there are m equations at each grid point (x_1, x_2, x_3); because of the spatial difference operators (δ_K and δ_K^2) these equations contain the dependent variables at x_K and at each of the two adjacent grid points in the x_K-direction. Consequently, the difference equations must be solved as an implicit system. It should be recognized that upon application at a successive number of grid points, x_K, each of Eqs. (81, 84, 85) generates a block-tridiagonal system of algebraic equations for $\bar{\phi}^{(k)}$ (i.e., $\bar{\phi}^*$, $\bar{\phi}^{**}$, or $\bar{\phi}^{***}$ for k = 1, 2, 3). After appropriate treatment of boundary conditions, each system can be solved efficiently using a standard block elimination method such as the matrix factorization method (see e.g., Ref. 61). The method used in the present study (Ref. 15) is closely related to the matrix factorization method and simply consists of Gaussian elimination for a tridiagonal matrix, but where the elements of the tridiagonal matrix are (m x m) submatrices rather than scalars, where m is the number of governing equations.

The solution procedure for a single time step is as follows:

(1) During the first step of the ADI procedure, Eq. (81) is applied at successive x_1-direction rows of grid points to provide one-dimensional

implicit systems of equations. These systems are generated by the operator $(\bar{A}^n/\Delta t - \bar{D}_1^n)$. The implicit systems can be arranged in block-tridiagonal form and solved as indicated previously. Since there are m governing equations, the block-tridiagonal systems have (m x m) square matrices as the block elements.

(2-3) The second and third steps are similar to (1) except that Eqs. (84) and (85) are applied along successive x_2 and x_3 direction rows of grid points to obtain implicit equations for $\bar{\phi}^{**}$ and $\bar{\phi}^{***}$, respectively.

The entire solution procedure requires only two levels of storage for each of the dependent variables, as well as storage for the block-tridiagonal coefficient matrix. Notice that only one-dimensional storage is required for the second and third steps in the procedure when Eqs. (84) and (85) are employed. (See Ref. 15 for further details).

Further Computational Details

Artificial Viscosity Terms

The optional artificial viscosity terms which were added to the difference equations may be useful in practical calculations to stabilize the method when boundary conditions are treated inaccurately, when coarse mesh spacing is used, or in the presence of discontinuities. The treatment of artificial viscosity terms used here (Ref. 15) is convenient but is considered provisional. Another combination of spatial difference formulas and/or artificial viscosity terms may eventually prove superior; however, this area requires further study.

It is known that some finite-difference approximations to first-order equations have viscosity-like truncation errors which serve to stabilize these difference schemes (Refs. 68 and 69). It seems advantageous, especially for computing viscous flows, to use a basic difference scheme which has no artificial viscosity and to add artificial viscosity terms in explicit form for optional use when needed for stability. The backward difference scheme with central differences for spatial derivatives is suitable from this standpoint, and this approach has been taken. The evaluation of artificial viscosity is

---

68. Roache, P. J.: On Artificial Viscosity. Journal of Computational Physics, Vol. 10, 1972, p. 169.
69. Roache, P. J.: Computational Fluid Dynamics. Hermosa Publishers, Albuquerque, New Mexico, 1972.

suggested by a consideration of the nondimensional model equation

$$u_i \frac{\partial \phi}{\partial x_i} = \frac{1}{Re} \frac{\partial^2 \phi}{\partial x_i^2} \tag{86}$$

which represents a balance between advection and diffusion. Roache (Refs. 68 and 69) has shown by a comparison with an exact solution of Eq. (86) that solutions obtained using central differences for the advection term are well behaved provided the mesh Reynold's number $Re_{\Delta x_i} = |u_i| \Delta x_i \, Re$ is ≤ 2, but that qualitative inaccuracies (associated with boundary conditions) may occur when $Re_{\Delta x_i} > 2$. This suggests the use of an artificial viscosity to ensure that the local effective mesh Reynolds number is no greater than two. Thus, Eq. (86) is replaced by

$$u_i \delta_i \phi = \left(\frac{1}{Re} + \epsilon_i \right) \delta_i^2 \phi \tag{87}$$

where

$$\epsilon_i = \begin{cases} \frac{1}{Re} \left(\frac{Re_{\Delta x_i}}{2} - 1 \right) & \text{if } Re_{\Delta x_i} > 2 \\ 0 & \text{if } Re_{\Delta x_i} \leq 2 \end{cases} \tag{88}$$

From Eq. (88), it is apparent that the artificial viscosity can be made to vanish by refining the mesh. Since the artificial viscosity is proportional to Δx_i, solutions will have first-order formal accuracy if $Re_{\Delta x_i} > 2$ but second-order accuracy if $Re_{\Delta x_i} \leq 2$. Strictly speaking, the overall method is second-order accurate since $Re_{\Delta x_i} \to 0$ as the mesh is refined. It should be remembered, however, that such asymptotic truncation error estimates are meaningful only for sufficiently small mesh size; whereas, in practical calculations of complex flows, mesh resolution capabilities have often, out of necessity, been strained. One virtue of the present formulation is that by isolating the artificial viscosity terms for comparison with other terms in the equations, a nonrigorous but plausible a posteriori indication of the first-order truncation error in a computed solution is available. It is, of course, obvious that Eq. (86), upon which the artificial viscosity is based, represents a gross simplification of the Navier-Stokes equations, and it is primarily for this reason that the present formulation of artificial viscosity terms is considered provisional.

Solution of the Difference Equations

It has been shown that difference equations for each row of grid points in the three-dimensional case can be written as a block-tridiagonal system having (m x m) square matrices as the block elements. For the chemically

reacting flow considered in this study the number of governing equations is as least seven ($m \geq 7$). Briley and McDonald (Ref. 15) have shown that it is possible to take advantage of the special nature of the coupling in the Navier-Stokes equations in order to reduce the size of the block elements in the tridiagonal system which must be solved in the solution procedure. It is only necessary to solve a block-tridiagonal system having $(m-2)\times(m-2)$ block elements as well as two simple tridiagonal systems. This can be seen by careful examination of Eqs. (1), (4), (5), (30) and (31). During the k^{th} step of the ADI procedure ($k = 1, 2, 3$), only derivatives with respect to x_k and t appear in the implicit difference equations. Therefore only the x_k-direction momentum equation is coupled to the remaining equations (1), (5), (30) and (31), since derivatives of the other two velocity components with respect to x_k do not appear in those equations.

The computational effort saved by solving one 5x5 block-tridiagonal and two simple tridiagonal systems rather than a 7x7 block-tridiagonal system can be estimated as shown in Ref. 15. If there are N grid points along a row being treated implicitly and ℓ coupled equations at each grid point, then the resulting block-tridiagonal system requires $(3N-2)(\ell^3 + \ell^2)$ arithmetic operations while $(5N-4)$ operations are required for the simple tridiagonal system (Ref. 61). Thus, for seven coupled equations the computational effort is approximately 1180N and for five coupled equations and two uncoupled equations it is about 460N. Therefore, the reduction to a system of five coupled equations and two uncoupled equations during each ADI step affords a considerable savings in computational effort. The results of Ref. 15 indicate that the computational effort per time step for the MINT method is only about twice that of most explicit methods, so that the gain in efficiency achieved by taking large time steps is real.

Nonuniform Grid Transformation

The accuracy of solutions computed with a given number of grid points can often be improved by using a nonuniform grid spacing to ensure that grid points are closely spaced in regions where the solution varies rapidly and widely spaced elsewhere. In a typical combustor flow situation, large gradients will occur near the combustor injection ports, in boundary layers on the walls, and in free shear layers resulting from the flow separation near injection ports. Transformations for the latter case have not been investigated in the present study. Boundary layers in a turbulent flow are treated using the wall function approximation, although occasionally some grid transformation may still be required near a wall.

An analytical coordinate transformation has been devised by Roberts (Ref. 70) which is a very effective means of introducing a nonuniform grid when the steep gradients occur near the computational boundaries. Suppose that N grid points are to be used in the range $X_1 \le X \le X_2$, and that steep gradients are anticipated in a region of thickness $\beta\,(X_2-X_1)$ near X_1. Then Roberts' transformation $X_T(X)$ is given by

$$X_T(X) = N+(N-1)\,\ln\left(\frac{X+b-c}{X+b-c}\right)\Big/\ln\left(\frac{b+a}{b-a}\right) \tag{89}$$

where $a = X_2-X_1$, $b^2 = a^2/(1-\beta)$, and $c = X_2$. The use of equally-spaced points in the transformed coordinate, X_T, ensures an adequate resolution of both the overall region $X_1 \le X \le X_2$ and the subregion $X_1 \le X < \beta(X_2-X_1)$. Derivatives with respect to the physical coordinate, X, are obtained from the following formulas:

$$\frac{\partial}{\partial X} = \frac{dX_T}{dX}\;\frac{\partial}{\partial X_T} \tag{90}$$

$$\frac{\partial^2}{\partial X^2} = \left(\frac{dX_T}{dX}\right)^2 \frac{\partial^2}{\partial X_T^2} + \frac{d^2X_T}{dX^2}\;\frac{\partial}{\partial X_T} \tag{91}$$

The use of three-point difference operators for X_T derivatives in Eqs. (90-91) produces similar operators for X derivatives. These X-derivative operators can be computed at the start of a calculation and stored, along with the X locations of grid points. No further consideration of the transformation is then required.

---

70. Roberts, G. O.: Computational Meshes for Boundary Layer Problems. Proceedings of the Second International Conference on Numerical Methods in Fluid Dyanmics, Springer-Verlag, New York, 1971, p. 171.

SECTION IV

RESULTS AND CONCLUSIONS

To evaluate the three-dimensional computational procedure described in the previous sections, comparisons were made between numerical predictions obtained from the MINT code and unpublished experimental data taken in a rectangular research combustor by the Pratt & Whitney Aircraft (P&WA) Combustion Group. The P&WA results consisted of temperature measurements taken with a shielded thermocouple probe and emission measurements (unburned hydrocarbons, nitric oxide, carbon monoxide, carbon dioxide) taken using gas sampling probes. No other suitable measurements were available for comparison. The P&WA research combustor is a rectangular duct with a cross section 1.5 by 3.0 in. and an overall length of about 10.0 in. The flame holder employed for the measurements described herein was a steel plate (0.25 in. thick) containing an array of eight (8) holes as shown in Fig. 3. The holes are 0.397 in. in diameter with 0.75 in. between hole centers. The P&WA combustion experiment employed prevaporized Jet-A aircraft fuel which was premixed with a preheated air stream. The nominal fuel composition was 85.9 weight percent carbon and 14.1 weight percent hydrogen with a molecular weight of 160.0; therefore, the nominal chemical formula for the fuel is $C_{11.44}H_{22.38}$. The fuel heat of combustion is approximately 4.3×10^7 joule/kg (18500 Btu/lbm), and a constant fuel specific heat (c_p) of 2510.0 joule/kg-$^\circ$K (0.6 Btu/lbm-$^\circ$R) was used in the present calculations. The air preheat temperature measured upstream of the flame holder was about 756°K (900°F); the total mass flow rate through the combustor was 2.86×10^{-2} kg/sec; and the fuel mass fraction was 0.0322.

The computational region boundaries considered in the present calculations are indicated by dashed lines in Fig. 3. In order to reduce the number of grid points required in the calculation the hole pattern was assumed to be periodic in the longitudinal direction, so that symmetry boundary conditions could be applied and only one-half of the inlet port need be considered, as shown in Fig. 3. The temperature measurements in the combustor indicate that this is a reasonable approximation.

The computational region and coordinate system are illustrated in Fig. 4. Figure 5 shows the sections (A, B, C) for which profile plots of axial velocity, temperature, and nitric oxide are presented. All predictions presented were made using a 17 by 9 by 17 grid (2601 grid points) for the x_1, x_2, x_3 directions, respectively. A maximum axial velocity (U_D) of 116.7 m/sec (382.9 ft/sec) was required to match the experimental mass flow rate. The reference length (L) for all coordinates is 0.01905 meters (0.75 in.). The calculation was initiated downstream of the flame holder assuming a mixture inlet temperature of 750°K and a pressure of 1.002×10^5

Pa (atmospheric pressure). Axial velocity profiles are given in Figs. 6, 7, and 8 at sections A, B, and C, respectively, for a series of axial stations. The qualitative characteristics of the jet expanding into the combustor seem to be represented quite reasonably. As one proceeds away from the inlet, the jet spreading is evident and reverse flow is clearly present behind the inlet-plane wall regions. Due to the large inlet velocity and the relatively small number of grid points employed in the calculation, cell Reynolds numbers in the axial direction became large so that significant artificial viscosity was required in the difference equations (see SECTION III). The presence of artificial viscosity in the present case resulted in a 25 percent increase in mass flux between the inlet and computational exit plane ($x_3 = 4.0$, nondimensional). This problem will be discussed further after presentation of the remaining results.

The equilibrium hydrocarbon chemistry assumption was not expected to be valid near the inlet port of the combustor under consideration. Therefore, an ad hoc ignition delay criterion was imposed on the solution to prevent unrealistically large temperature gradients from occurring near the inlet. This was accomplished in the present numerical procedure by specifying the pseudo-kinetic rate constant, k_{HC}, as a function of axial distance from the inlet plane. The effect of the specified ignition delay on the port-centerline axial temperature variations is shown in Fig. 9, along with experimental measurements at four axial stations. The gas temperature of 756°K (900°F) originally quoted upstream of the flame holder is shown on Fig. 9. Subsequent thermocouple measurements with similar flame holders have shown that this temperature measurement is probably in error and should be approximately 1030°K (1400°F), which is consistent with the measurement at $x_3 = 0.167$. Since the equilibrium temperatures achieved downstream are predicted correctly (Fig. 9), it seems likely that the actual temperature far upstream of the flame holder is 756°K. The higher temperature of 1030°K believed to be present upstream of the flame holder may be attributed to heat transfer through the flame holder from the combustion zone to the gas mixture upstream of the flame holder, and possibly to combustion upstream of the flame holder. Unfortunately, this information was acquired subsequent to completion of the present numerical calculations, and the reported predictions are thus based on an incorrect inlet temperature. Proper treatment of the flame holder boundary conditions would require additional information regarding the heat transfer or surface temperature of the flame holder. If there are significant energy losses through the flame holder, these would not be correctly represented by the adiabatic wall conditions actually employed in the calculations. However, the adiabatic wall conditions are consistent with the inlet temperature of 756°K used in the calculations. One further consideration affecting the temperature predictions is the error in mass flux attributable to artificial viscosity.

Errors in mass flux associated with density would be reflected in the temperature through the equation of state. Furthermore, since the actual hydrocarbon combustion is a nonequilibrium process, only qualitative comparisons are warranted between the predictions and measurements where chemical equilibrium does not exit. In fact, the difference between computed and measured axial temperature variation in Fig. 9 is believed to be due mainly to the nonequilibrium nature of the combustion chemistry, and thus accents the shortcomings of an equilibrium chemistry model.

Nondimensional temperature profiles are presented in Figs. 10 to 12 at sections A, B, and C, respectively, for a series of axial stations. The presence of artificial viscosity (in the axial direction) in both the species and energy equations may have distorted the transverse temperature profiles, since outside the jet boundaries artificial diffusion is significant compared to convection. Representative experimental temperature measurements and the corresponding predictions are shown in Figs. 13 to 15. An axial translation of two predicted temperature profiles (Figs. 14 and 15) indicates reasonable qualitative agreement with the measured profiles. This translation is an a posteriori attempt to compensate for the incorrect pseudo-kinetic rate constant employed in the calculations. The qualitative agreement displayed in Figs. 14 and 15 provides some confidence in the numerical procedure and justification for further improvement of the physical models. Also, the distortion due to excessive artificial viscosity is a problem requiring further study before quantitatively meaningful comparisons can be made. Both Figs. 9 and 15 show good agreement between prediction and experiment once chemical equilibrium has been achieved.

Only a limited number of nitric oxide (NO) concentration measurements were made in the combustor under consideration. Since the NO concentration is sensitive to the temperature history of a fluid particle, the only comparison presented is that where equilibrium temperatures have been achieved. The predicted NO concentrations (Fig. 16) are significantly lower than measured values, which may be partly attributed to the simplifying assumptions made in the present NO chemistry analysis (SECTION II) and to nonequilibrium chemistry effects on combustor temperatures. Furthermore, NO concentrations of only several ppm are difficult to measure accurately.

The present numerical results demonstrate both the basic integrity of the computational procedure developed under the present study and the capability of the MINT code to perform calculations of three-dimensional combusting flows with recirculation. The need for improvement of the differencing scheme is apparent because of distortion in the predictions

due to excessive artificial viscosity. Experience at UTRC with the FREP computer code (Ref. 49) has shown that a two-equation transport model of turbulence offers significant advantages over a mixing length, eddy viscosity turbulence model in view of the considerable difficulty of specifying a mixing length distribution in a three-dimensional recirculating flow. The need for a simple nonequilibrium hydrocarbon chemistry model such as one based on the single step reaction mechanism, Eq. (29), is also evident. Work on alternate difference formulas for problems with large cell Reynolds numbers and on a two-equation turbulence model will be carried out under Phase II of the present contract.

APPENDIX A: GENERALIZED COORDINATE SYSTEM

In the system of orthogonal curvilinear coordinates x_1, x_2, x_3 with metric coefficients h_1, h_2, h_3 the differential element of arc length da is given by

$$(da)^2 = (h_1 dx_1)^2 + (h_2 dx_2)^2 + (h_3 dx_3)^2 \tag{92}$$

The vector operations necessary for deriving the governing differential equations in the present coordinate system from the vector equations (1-5) are given below. Let i_1, i_2, and i_3 be unit vectors in the coordinate directions x_1, x_2, x_3, respectively. Then the gradient operator is

$$\nabla \equiv \frac{\vec{i}_1}{h_1}\frac{\partial}{\partial x_1} + \frac{\vec{i}_2}{h_2}\frac{\partial}{\partial x_2} + \frac{\vec{i}_3}{h_3}\frac{\partial}{\partial x_3} \tag{93}$$

and a general vector $\vec{v}$ is

$$\vec{v} = \vec{i}_1 v_1 + \vec{i}_2 v_2 + \vec{i}_3 v_3 \tag{94}$$

The divergence of a vector is given by

$$\nabla \cdot \vec{v} = \frac{1}{h_1 h_2 h_3}\left[\frac{\partial}{\partial x_1}(h_2 h_3 v_1) + \frac{\partial}{\partial x_2}(h_1 h_3 v_2) + \frac{\partial}{\partial x_3}(h_1 h_2 v_3)\right] \tag{95}$$

The divergence of a symmetric tensor $\bar{\bar{t}}$ with components t_{ij} is a vector with the following components (Ref. 18):

$$(\nabla \cdot \bar{\bar{t}})_1 = \frac{1}{h_1 h_2 h_3}\left[\frac{\partial}{\partial x_1}(h_2 h_3 t_{11}) + \frac{\partial}{\partial x_2}(h_1 h_3 t_{12}) + \frac{\partial}{\partial x_3}(h_1 h_2 t_{13})\right] + \frac{t_{12}}{h_1 h_2}\frac{\partial h_1}{\partial x_2} + \frac{t_{13}}{h_1 h_3}\frac{\partial h_1}{\partial x_3} - \frac{t_{22}}{h_1 h_2}\frac{\partial h_2}{\partial x_1} - \frac{t_{33}}{h_1 h_3}\frac{\partial h_3}{\partial x_1} \tag{96}$$

$$(\nabla \cdot \bar{\bar{t}})_2 = \frac{1}{h_1 h_2 h_3}\left[\frac{\partial}{\partial x_1}(h_2 h_3 t_{12}) + \frac{\partial}{\partial x_2}(h_1 h_3 t_{22}) + \frac{\partial}{\partial x_3}(h_1 h_2 t_{23})\right] + \frac{t_{23}}{h_2 h_3}\frac{\partial h_2}{\partial x_3} + \frac{t_{12}}{h_1 h_2}\frac{\partial h_2}{\partial x_1} - \frac{t_{33}}{h_2 h_3}\frac{\partial h_3}{\partial h_2} - \frac{t_{11}}{h_1 h_2}\frac{\partial h_1}{\partial x_2} \tag{97}$$

$$(\nabla\cdot\bar{\bar{f}})_3 = \frac{1}{h_1 h_2 h_3}\left[\frac{\partial}{\partial x_1}(h_2 h_3 f_{13}) + \frac{\partial}{\partial x_2}(h_1 h_3 f_{23}) + \frac{\partial}{\partial x_3}(h_1 h_2 f_{33})\right] + \frac{f_{13}}{h_1 h_3}\frac{\partial h_3}{\partial x_1} + \frac{f_{23}}{h_2 h_3}\frac{\partial h_3}{\partial x_2} - \frac{f_{11}}{h_1 h_3}\frac{\partial h_1}{\partial x_3} - \frac{f_{22}}{h_2 h_3}\frac{\partial h_2}{\partial x_3} \quad (98)$$

The foregoing relationships are substituted into the equations (1) to (5) to obtain the governing equations in the generalized coordinate system. The axisymmetric coordinates are obtained by taking $h_2 = r$, where r is the radial distance from the axis of symmetry and x_2 is the angular coordinate (Fig. 1).

An analysis for determination of the metric coefficients h_1 and h_3 based on the two-dimensional incompressible potential flow in a duct has been developed by Anderson (Ref. 71), together with a computer program to implement the analysis. The method utilizes orthogonal streamlines and velocity potential lines as the coordinate lines for constant x_1 and x_3, respectively. Therefore, it follows from potential flow theory that x_1 and x_3 are solutions of Laplace's equation, i.e., $\nabla^2 x_1 = \nabla^2 x_3 = 0$. By an appropriate normalization of x_1 and x_3, Anderson (Ref. 71) has shown that the metric coefficients h_1 and h_3 can be made to satisfy the relationship $h_1 = h_3 = 1/U_I$, where U_1 is the nondimensional inviscid velocity. Anderson's solution procedure is based on a representation of the boundaries of the inviscid flow region by a large number of straight line segments, thus forming a many-sided polygon. The Schwartz-Christoffel conformal transformation is then employed to transform this polygon into a semi-infinite plane, where the potential flow solution is known. An iterative numerical solution for the transformed locations of the various nodal points (corners of the polygon), followed by the known inverse Schwartz-Christoffel transformation, provides the inviscid potential flow and coordinate system for the desired geometry. Uniform-velocity boundary conditions are specified at the inlet and exit planes of the inviscid flow region. If necessary or desired, the inviscid flow region can be extended upstream and/or downstream of the region to be used in the viscous solution. This computer program has been employed by Briley and McDonald (Ref. 72) to obtain an orthogonal curvilinear coordinate system for computation of the three-dimensional subsonic flow in curved passages. The analysis of Anderson (Ref. 71) can be implemented within the framework of this study whenever it is required.

---

71. Anderson, O. L.: User's Manual for a Finite-Difference Calculation of Turbulent Swirling Compressible Flow in Axisymmetric Ducts with Struts and Slot Cooled Walls. USAAMRDL-TR-74-50, Vol. I, 1974.

72. Briley, W. R. and H. McDonald: Computation of Three-Dimensional Turbulent Subsonic Flow in Curved Passages. United Technologies Research Center Report No. R75-911596-8, March 1975.

TABLE I. Chemical Rate Constants

$k = A\ T^N \exp(-B/RT)$ *

REACTION	FORWARD RATE			REVERSE RATE		
	A	B	N	A	B	N
$N_2 + O \rightleftharpoons NO + N$	1.36×10^{14}	75400	0	3.10×10^{13}	334	0
$N + O_2 \rightleftharpoons NO + O$	6.43×10^{9}	6250	1.0	1.55×10^{9}	38640	1.0
$N + OH \rightleftharpoons NO + H$	4.22×10^{13}	0.0	0	1.64×10^{14}	48600	0

*Units are cm, cal, °K, g-mole, sec

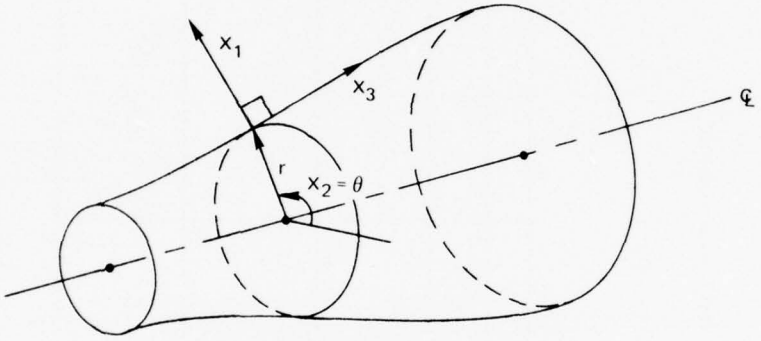

Figure 1. General axisymmetric combustor geometry.

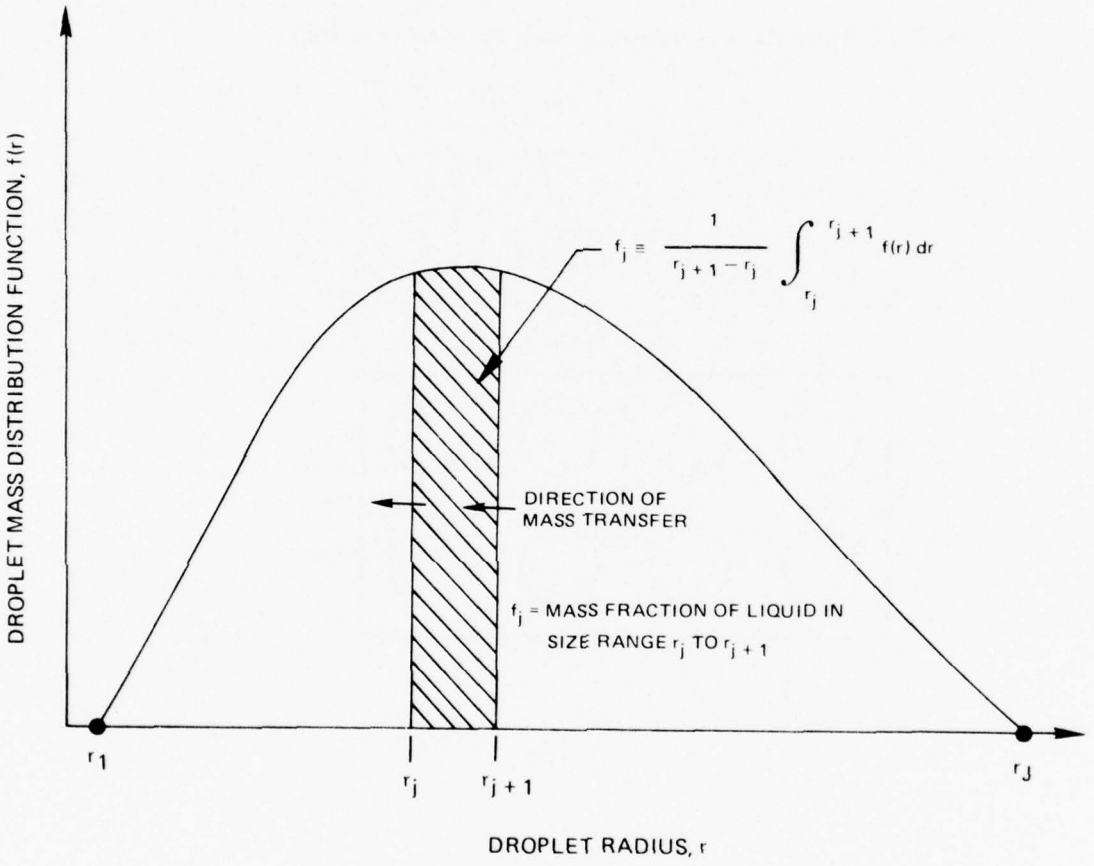

Figure 2. Schematic representation of particle fraction.

R10-85-3

NOTE: COMPUTATIONAL BOUNDARIES DENOTED BY DASHED LINES

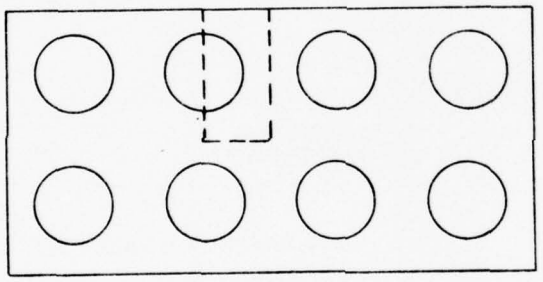

Figure 3. Experimental flameholder configuration for three dimensional rectangular combustor

R11-32-2

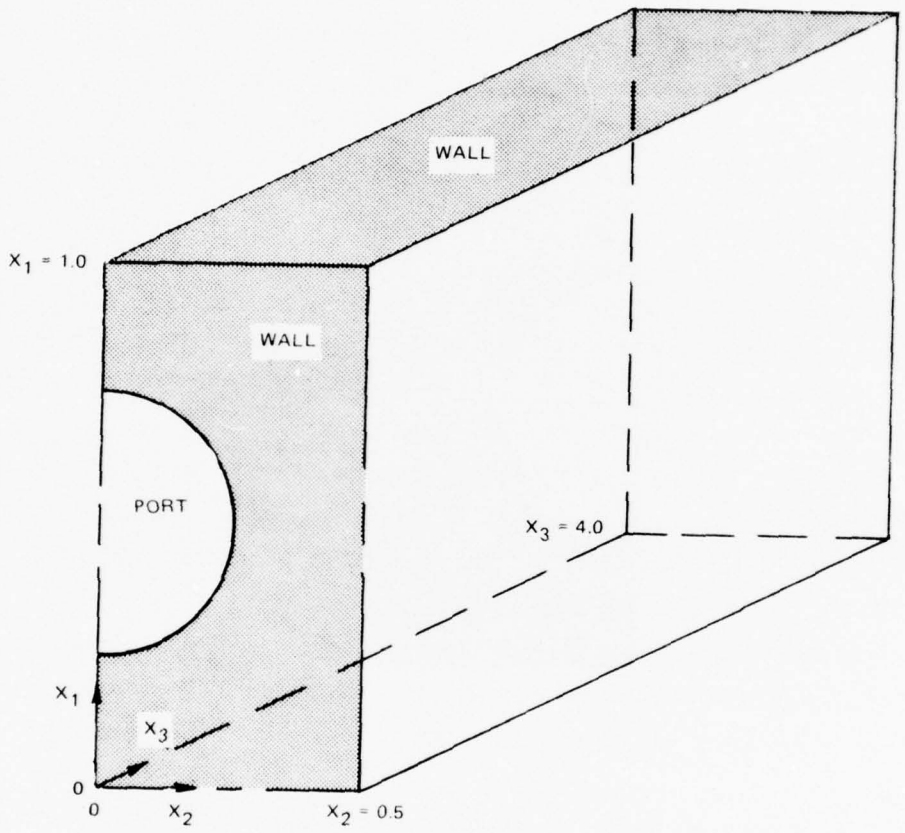

Figure 4. Computational region and coordinate system for three dimensional rectangular combustor

R11-32-3

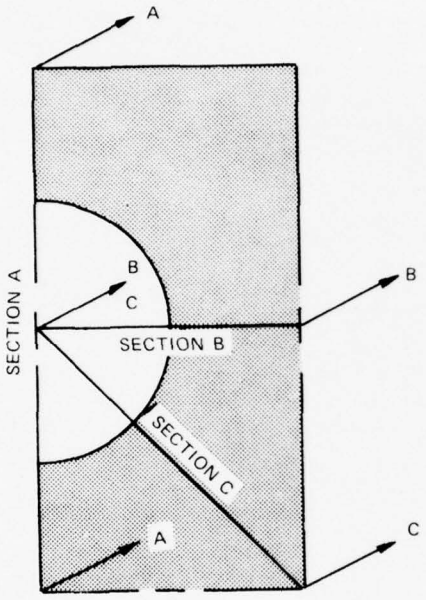

Figure 5. Cross flow plane sections A,B, and C for profile plots

R11-32-4

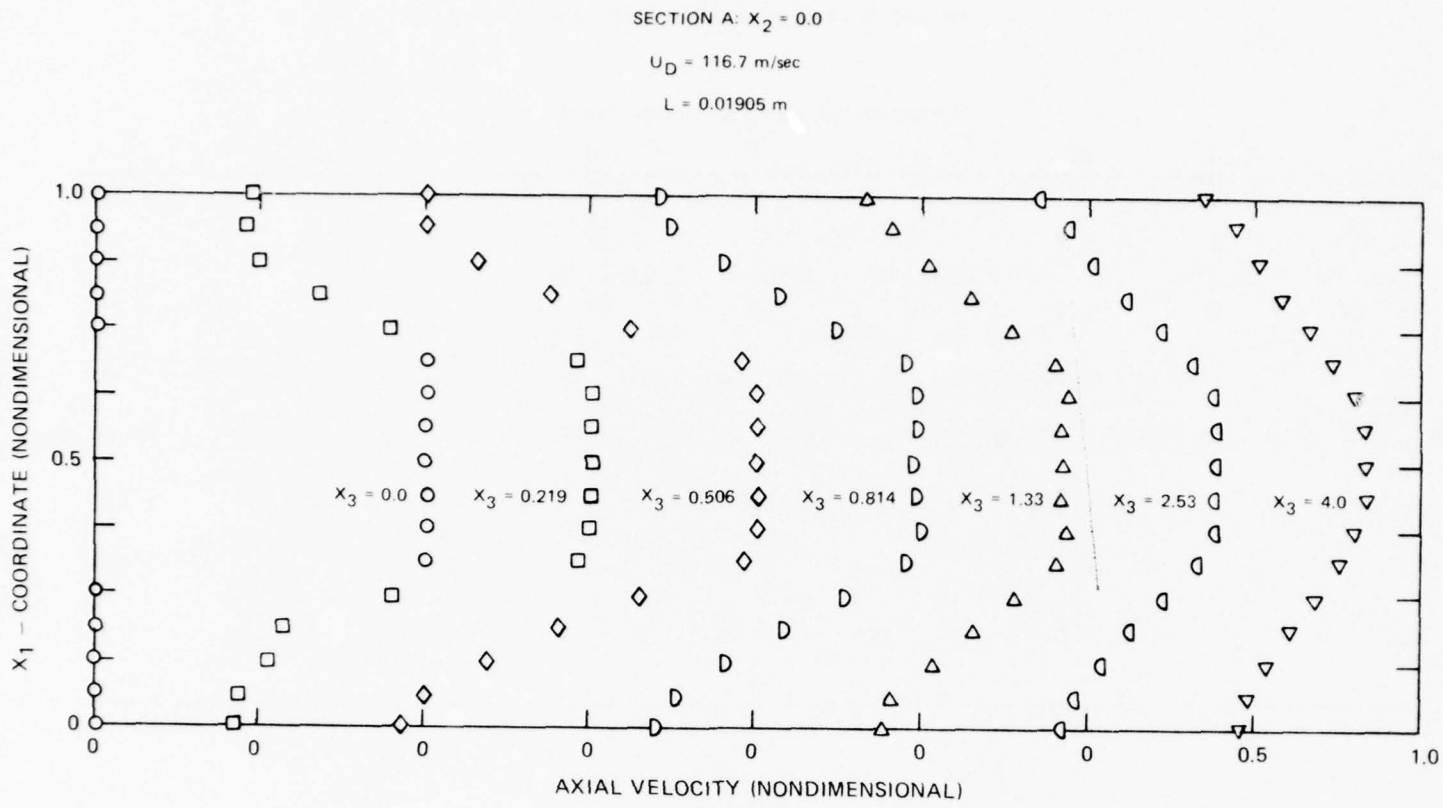

Figure 6. Nondimensional axial velocity profiles

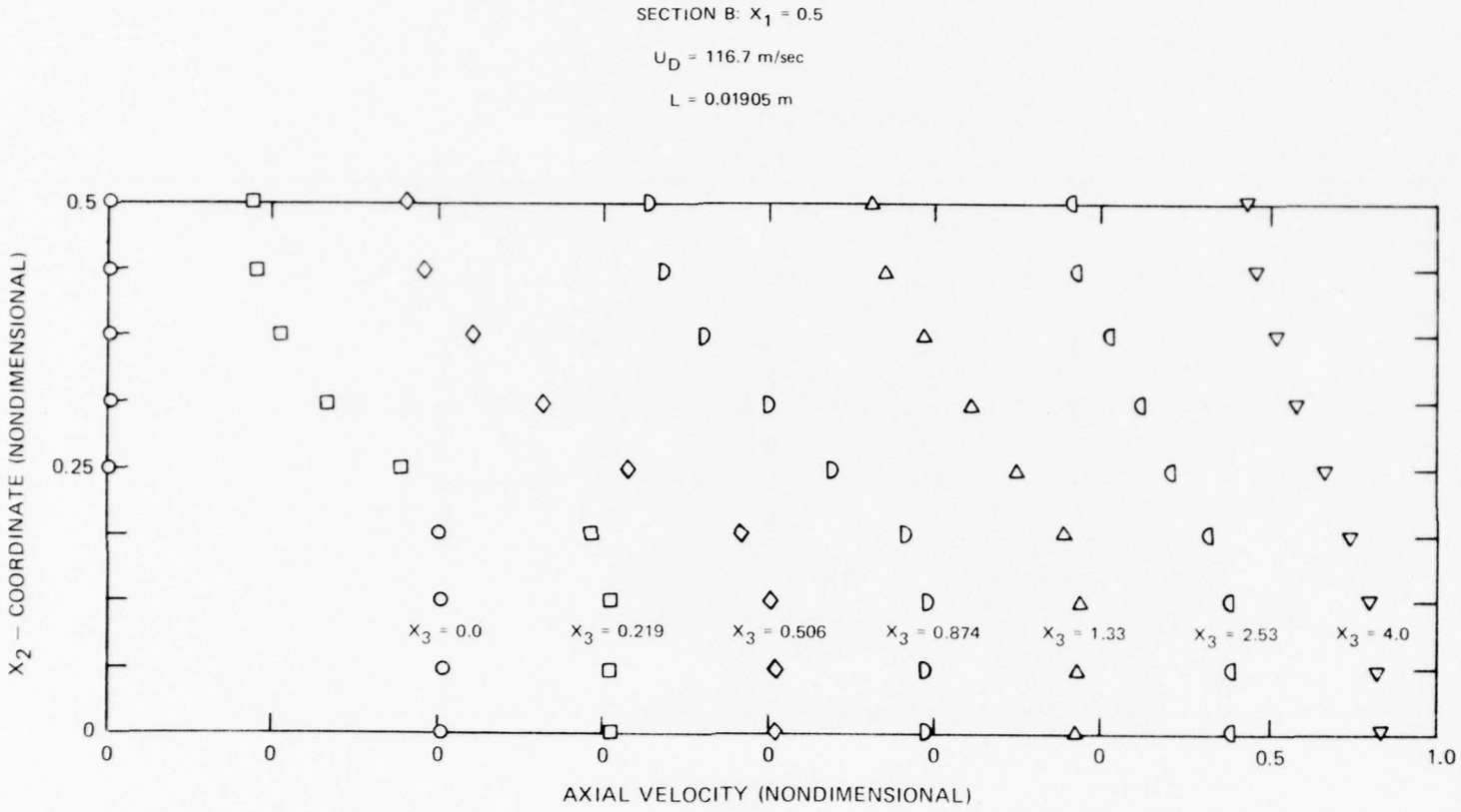

Figure 7. Nondimensional axial velocity profiles

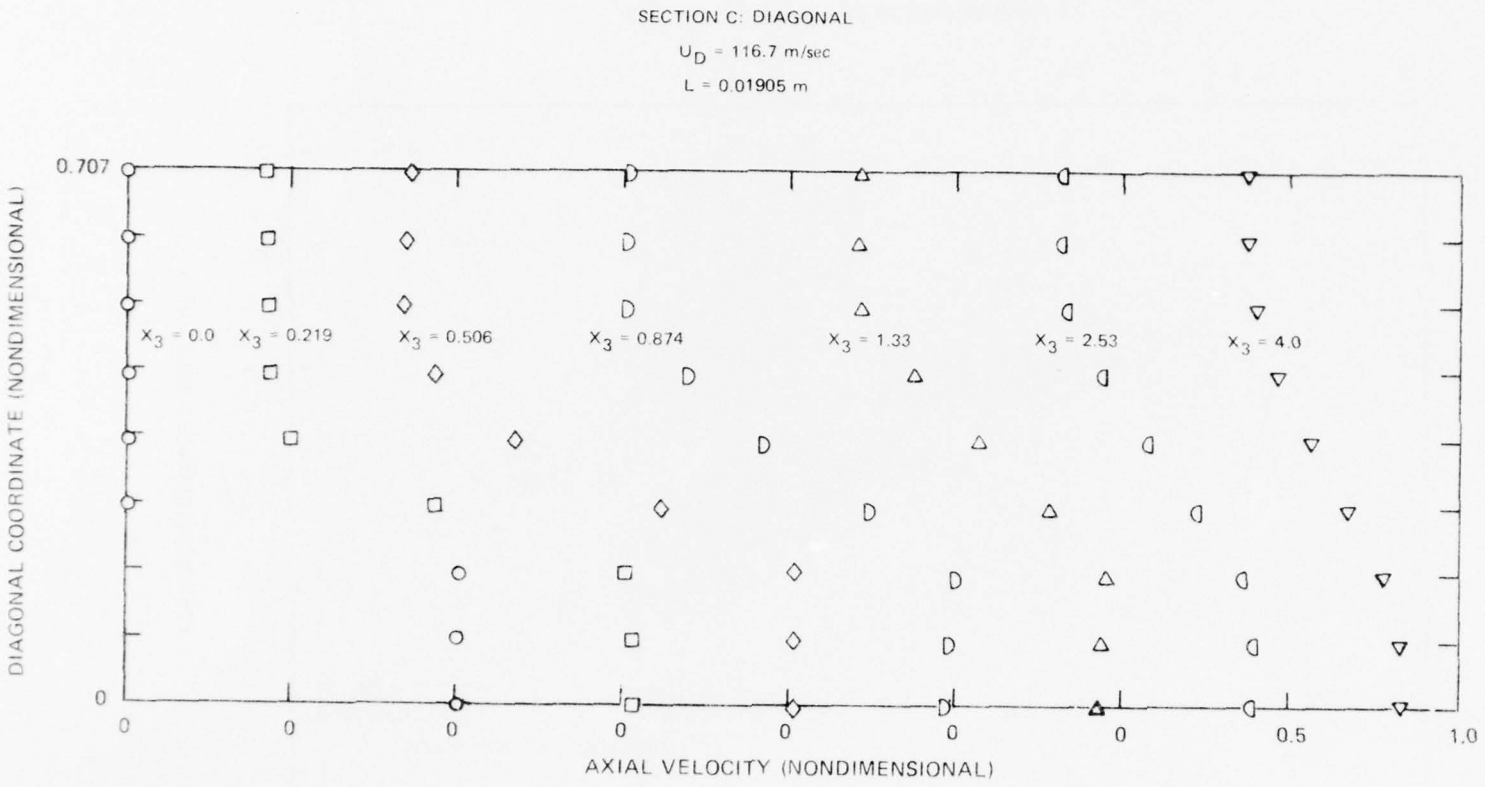

Figure 8. Nondimensional axial velocity profiles

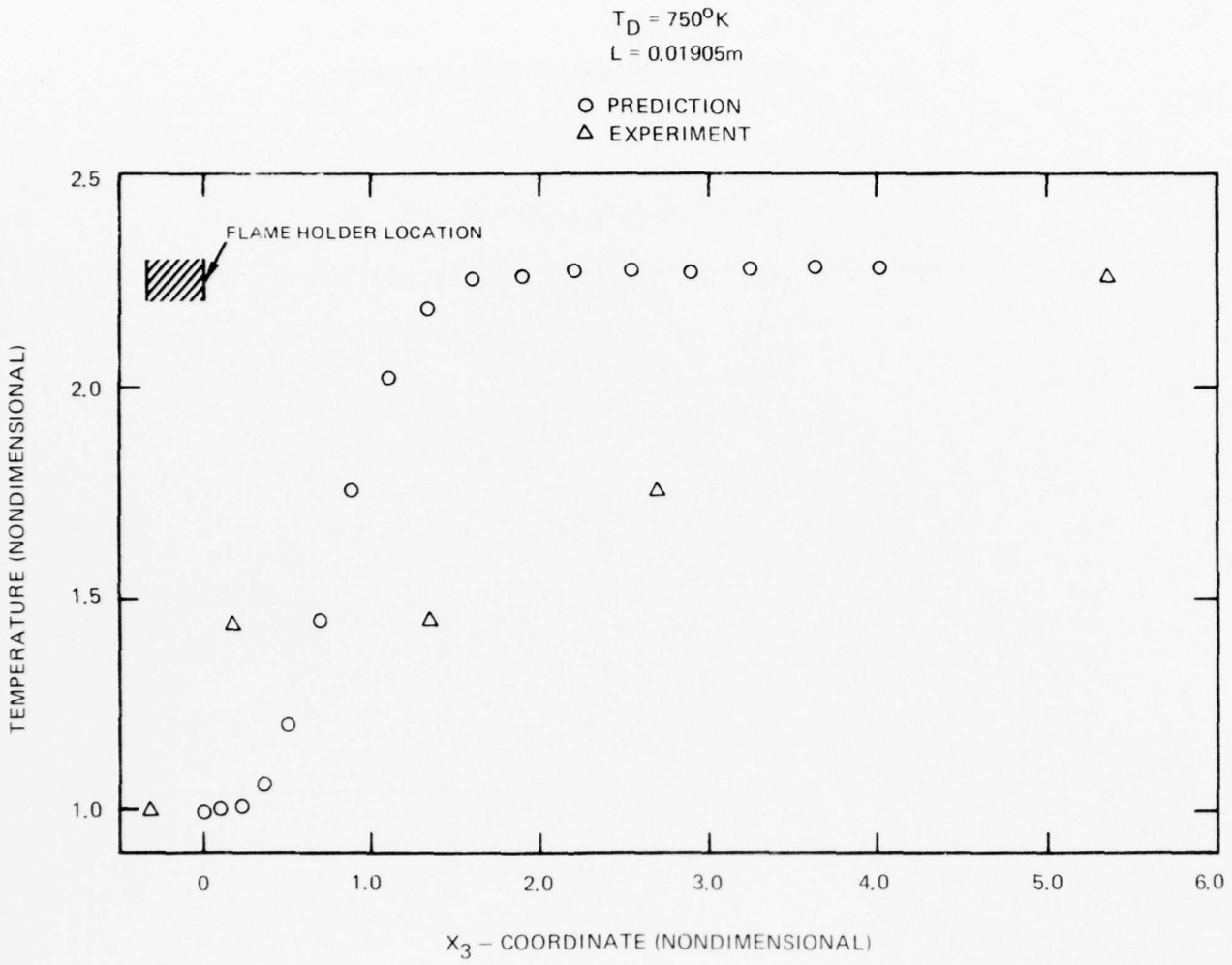

Figure 9. Axial variation of temperature along port centerline ($x_1 = 0.5$, $x_2 = 0.0$)

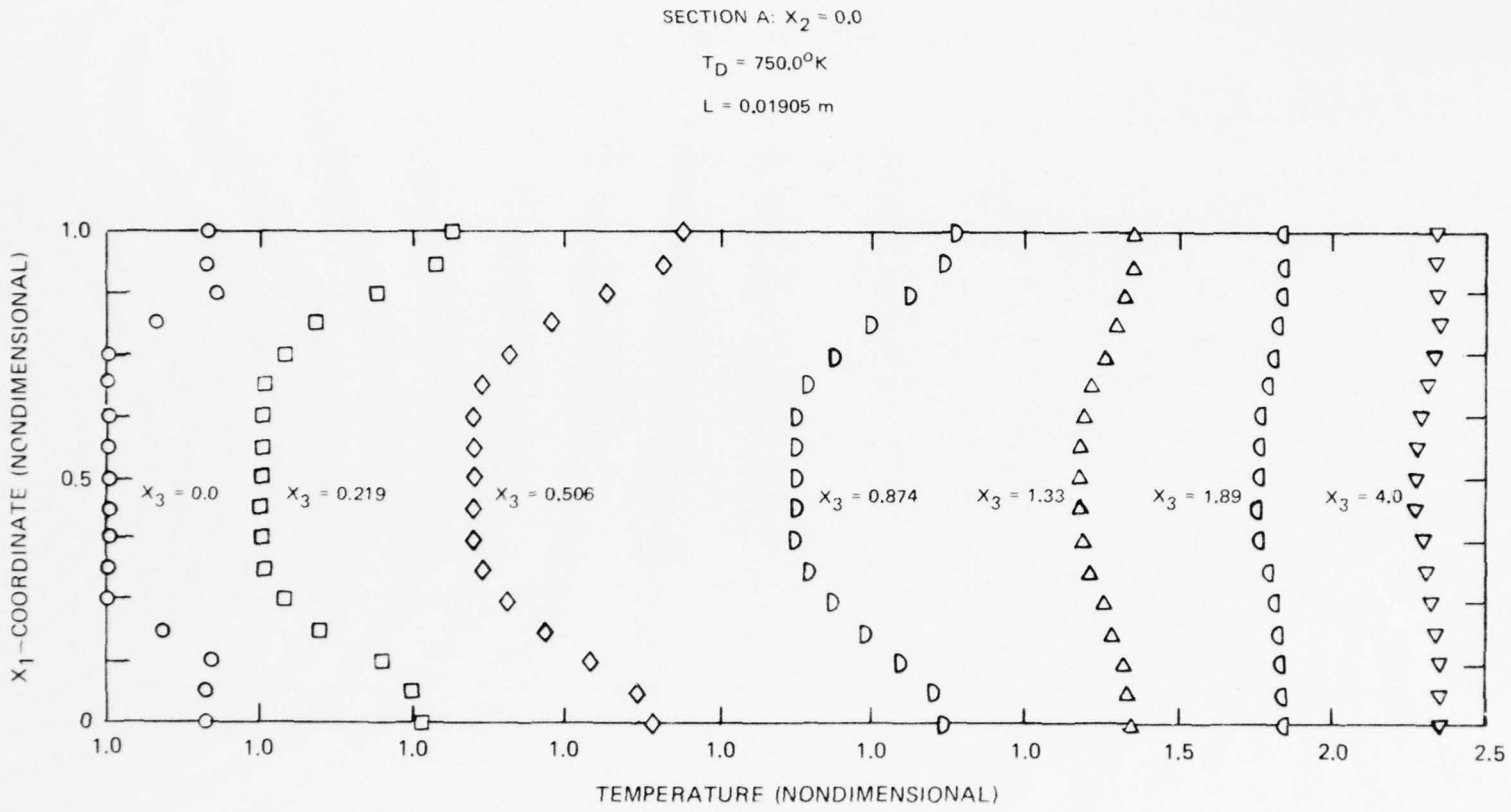

Figure 10. Nondimensional temperature profiles

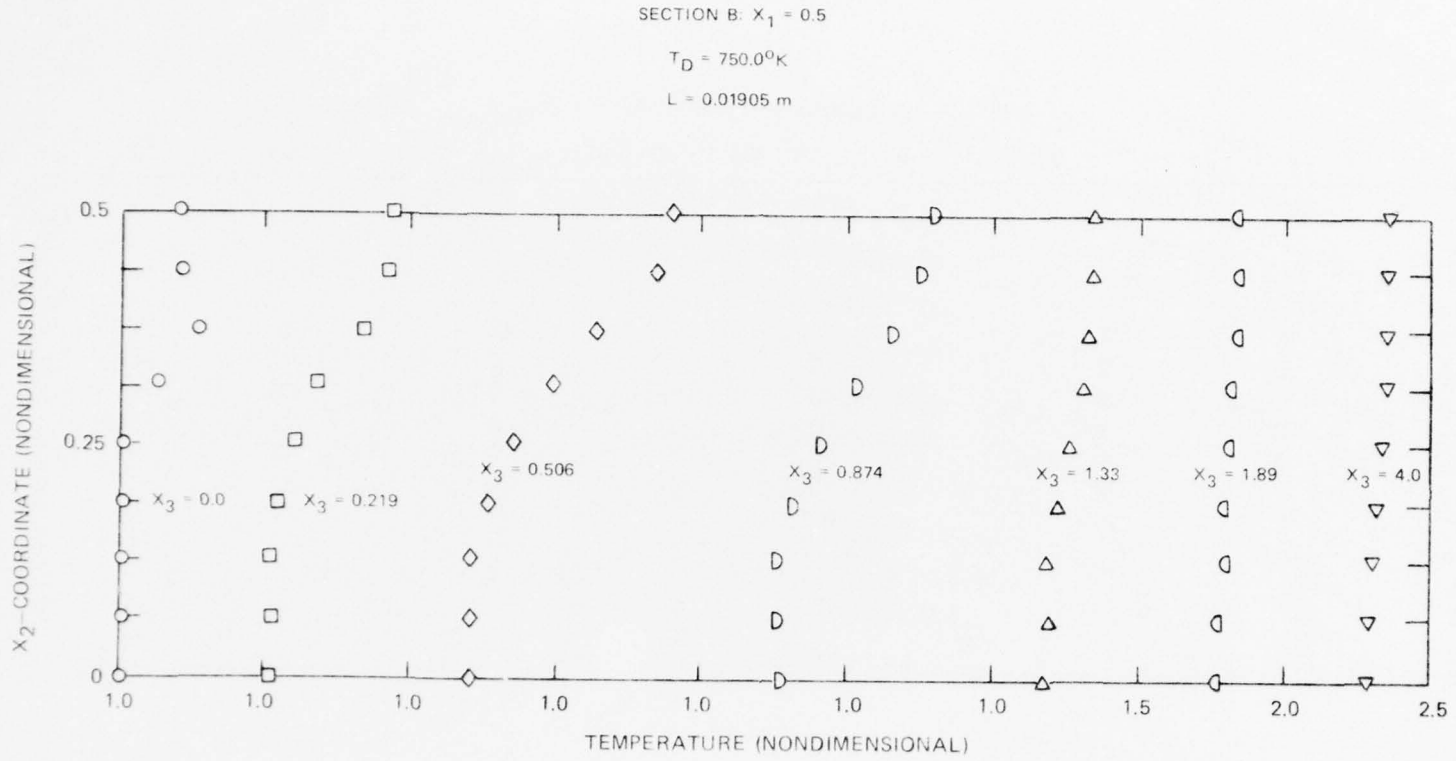

Figure 11. Nondimensional temperature profiles

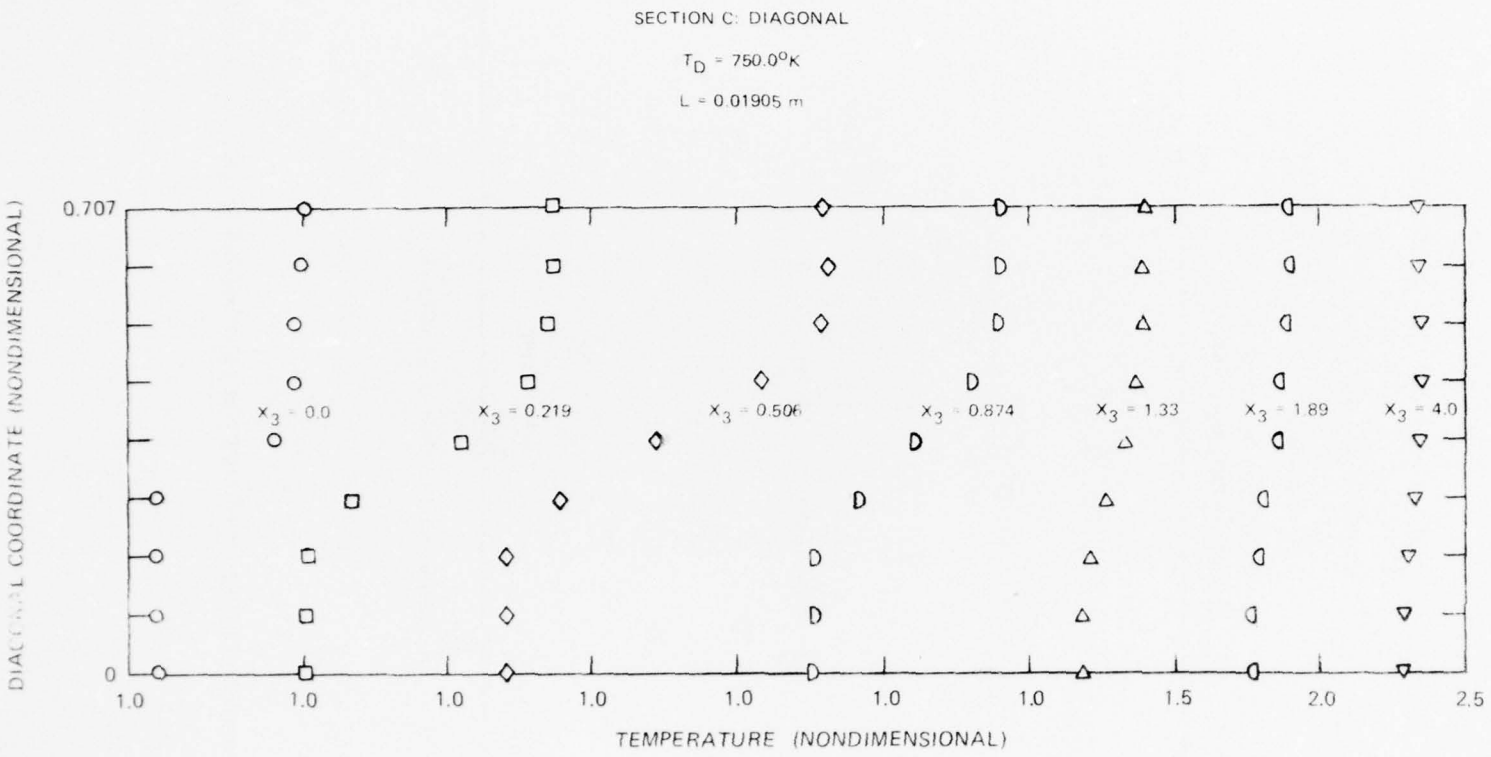

Figure 12. Nondimensional temperature profiles

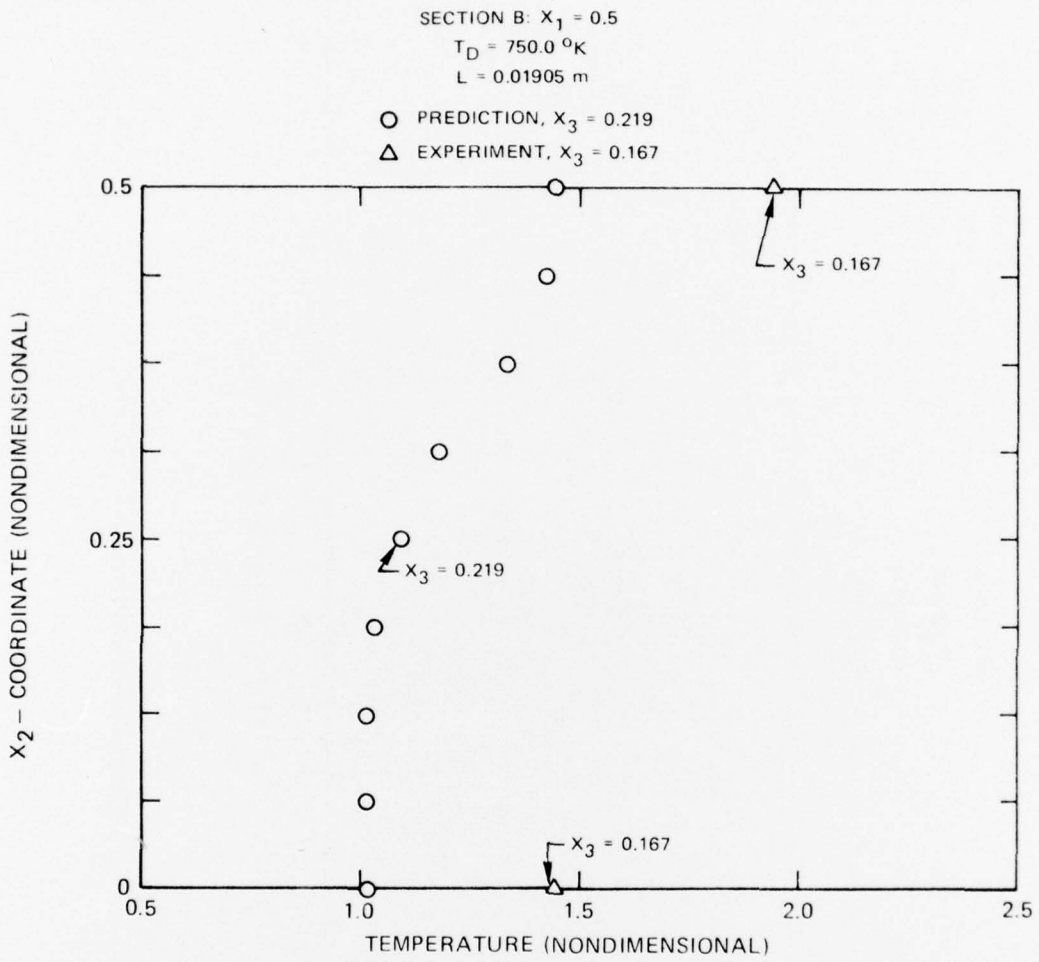

Figure 13. Comparison between predicted and experimental temperature profiles.

R11-35-1

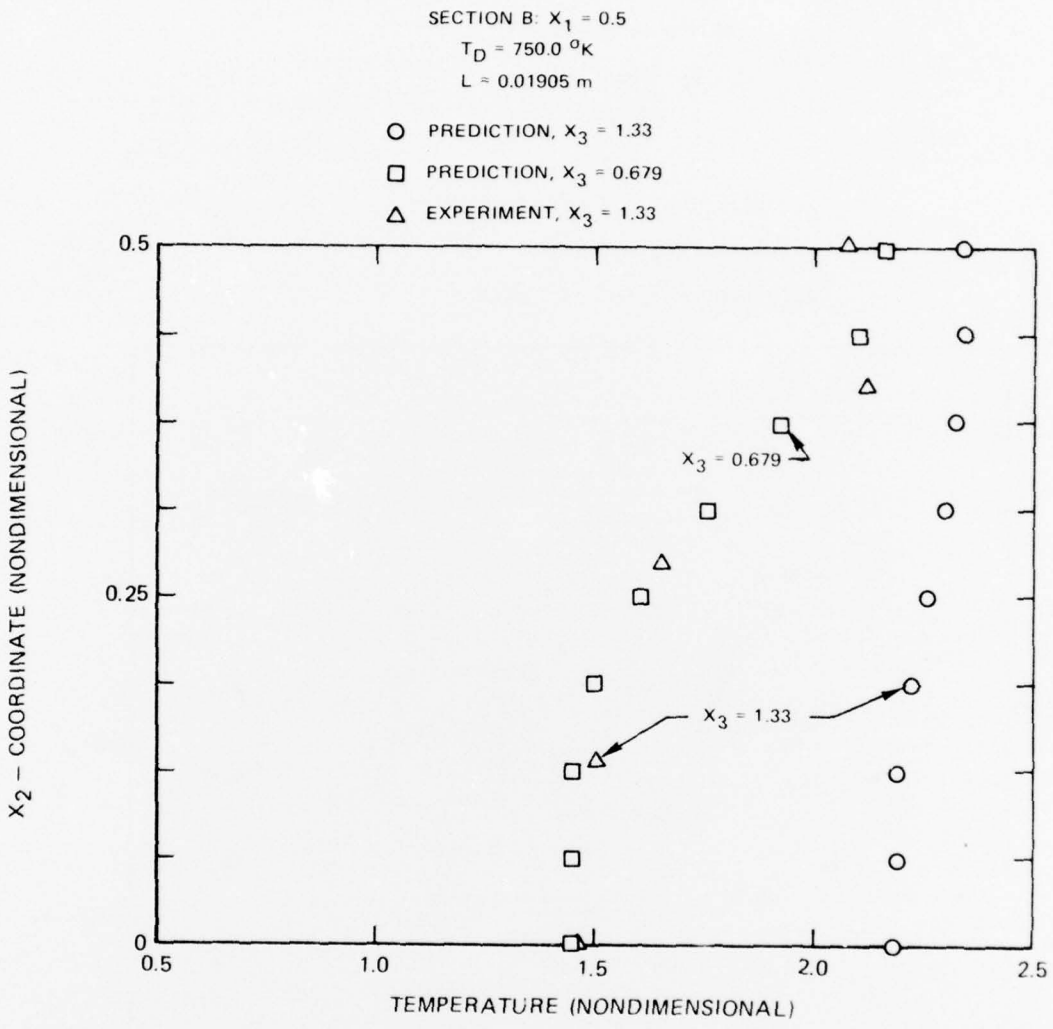

Figure 14. Comparison between predicted and experimental temperature profiles.

R11-35-3

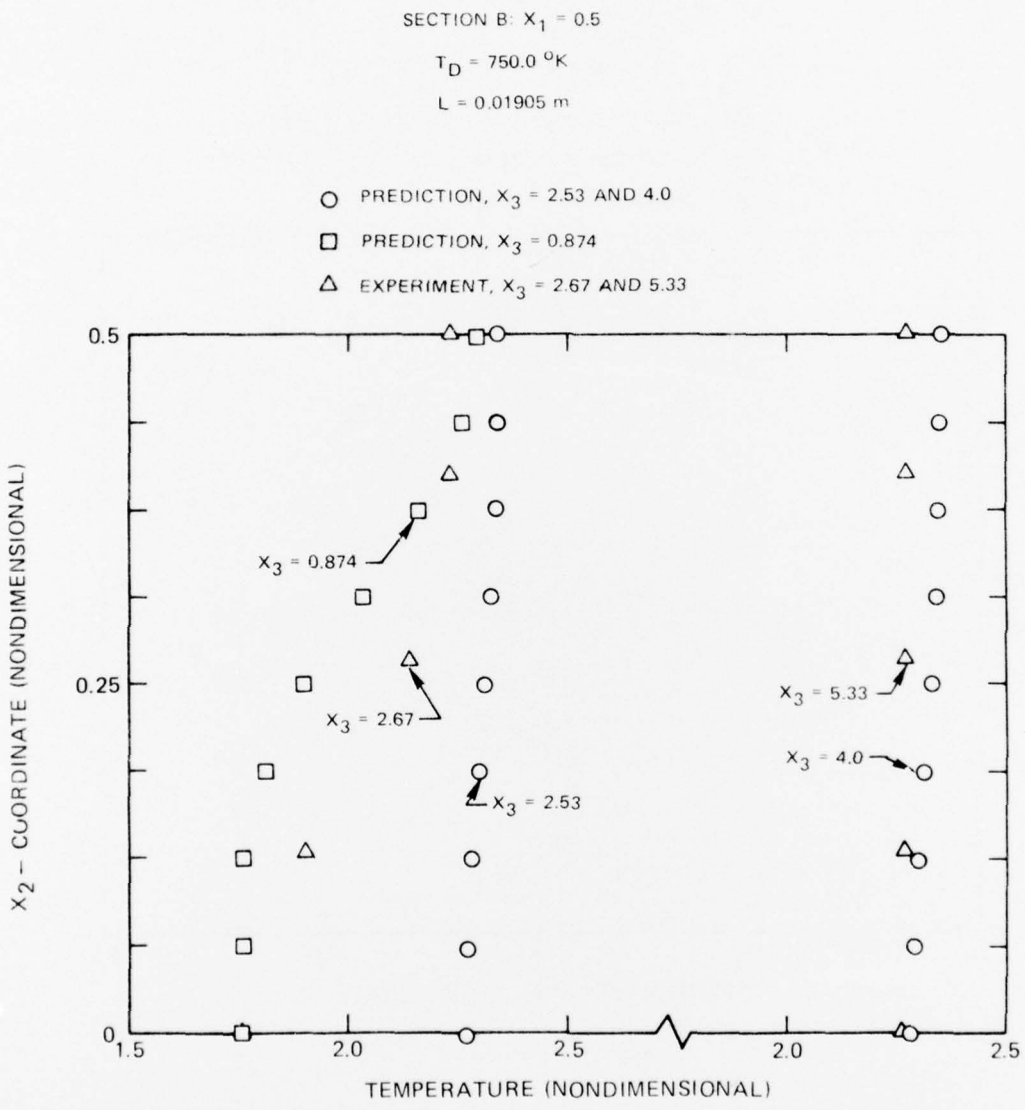

Figure 15. Comparison between predicted and experimental temperature profiles.

R11-35-2

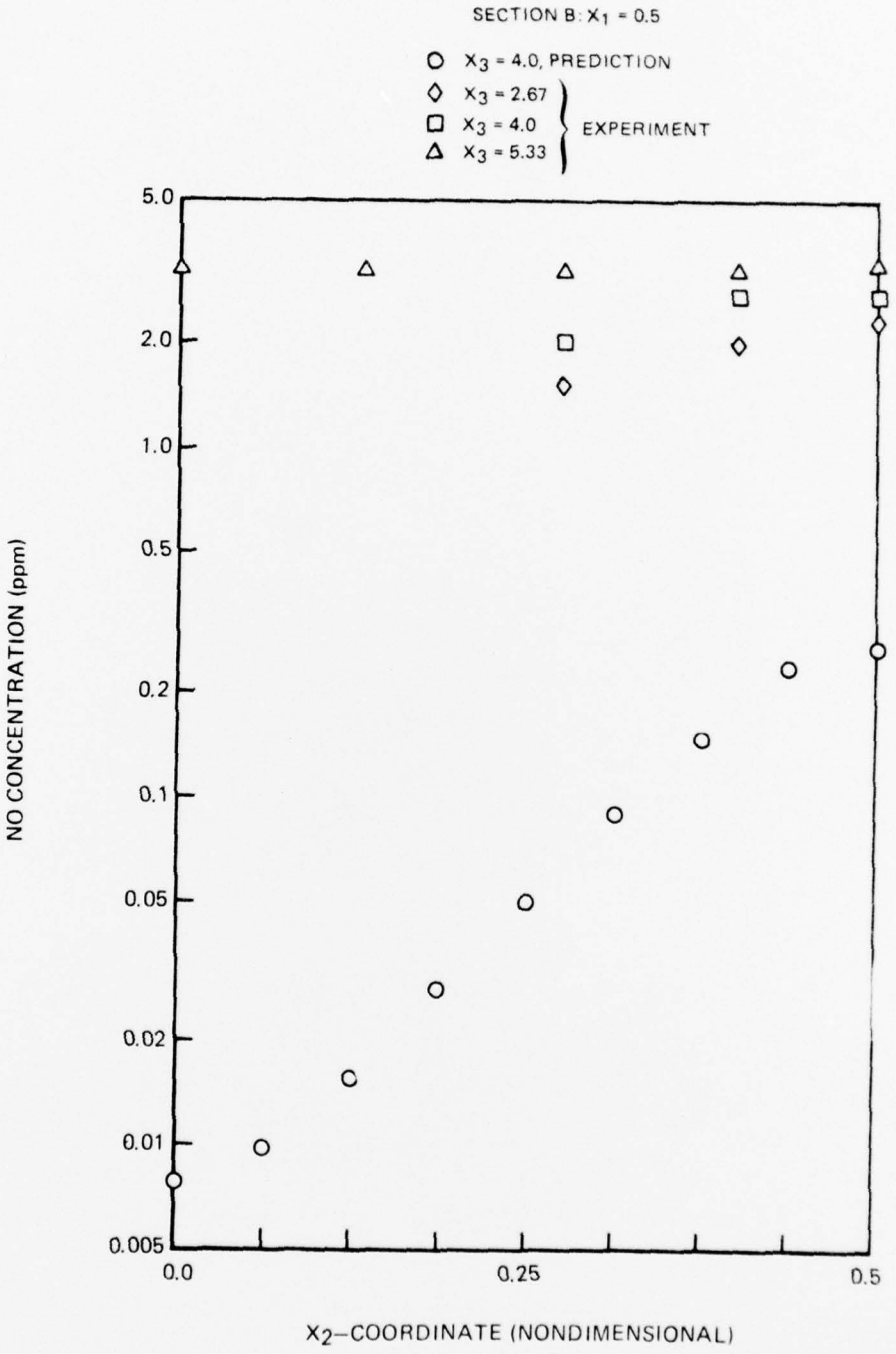

Figure 16. Comparison between predicted and experimental nitric oxide (NO) concentration profiles

REFERENCES

1. Beer, J. M. and N. A. Chigier: Stability and Combustion Intensity of Pulverized Coal Flames - Effect of Swirl and Impingement. Journal of the Institute of Fuel, December 1969.

2. Beer, J. M. and W. Leucker: Turbulent Flames in Rotating Flow Systems. Paper No. Inst. F-NAFTC-7, North American Fuel Technology Conference, Ottawa, Canada, 1970.

3. Beer, J. M. and J. B. Lee: The Effects of Residence Time Distribution on the Performance and Efficiency of Combustors. The Combustion Institute, 1965, pp. 1187-1202.

4. Marteney, P. J.: Analytical Study of the Kinetics of Formation of Nitrogen Oxide in Hydrocarbon - Air Combustion. Combustion Science and Technology, Vol. 1, 1970, pp. 37-45.

5. Fletcher, R. S. and J. B. Heywood: A Model for Nitric Oxide Emission from Aircraft Gas Turbine Engines. AIAA Paper 71-123, 1971.

6. Hammond, D. C., Jr. and A. M. Mellor: Analytical Predictions of Emissions from and Within an Allison J-33 Combustor. Combustion Science and Technology, Vol. 6, 1973, pp. 279-286.

7. Hammond, D. C., Jr. and A. M. Mellor: Analytical Calculations for the Performance and Pollutant Emissions of Gas Turbine Combustors. Combustion Science and Technology, Vol. 4, 1971, pp. 101-112.

8. Roberts, R., L. D. Aceto, R. Keilback, D. P. Teixeira, and J. M. Bonnell: An Analytical Model for Nitric Oxide Formation in a Gas Turbine Combustion Chamber. AIAA Paper No. 71-715, 1971.

9. Mosier, S. A., R. Roberts, and R. E. Henderson: Development and Verification of an Analytical Model for Predicting Emissions from Gas Turbine Engine Combustors During Low Power Operation. 41st Meeting Propulsion and Energetics Panel of AGARD, 1973.

10. Edelman, R. and C. Economos: A Mathematical Model for Jet Engine Combustor Pollutant Emissions. AIAA Paper No. 71-714, 1971.

11. Gosman, A. D., W. M. Pun, A. K. Runchal, D. B. Spalding, and M. Wolfshtein: Heat and Mass Transfer in Recirculating Flows. Academic Press, New York, 1969.

12. Anasoulis, R. F.: Computations of the Flow in a Combustor. United Aircraft Research Laboratories Report K110885-1, November 1971.

13. Anasoulis, R. F., H. McDonald and R. C. Buggeln: Development of a Combustor Flow Analysis, Part I: Theoretical Studies. Air Force Aero Propulsion Laboratory Report AFAPL-TR-73-98, Part I, January 1974.

14. Patankar, S. V. and D. B. Spalding: A Computer Model for Three-Dimensional Flow in Furnaces. Fourteenth Symposium (International) on Combustion, The Combustion Institute, 1973, pp. 606-614.

15. Briley, W. R. and H. McDonald: An Implicit Numerical Method for the Multidimensional Compressible Navier-Stokes Equations. United Aircraft Research Laboratories Report M911363-6, November 1973.

16. Bird, R. B., W. E. Stewart, and E. N. Lightfoot: Transport Phenomena. Wiley, New York, 1960.

17. Williams, F. A.: Combustion Theory. Addison-Wesley, Reading, Massachusetts, 1965.

18. Emmons, H. W., ed.: Fundamentals of Gas Dynamics. High Speed Aerodynamics and Jet Propulsion, Vol. 3, Princeton University Press, Princeton, N. J., 1958.

19. Launder, B. E. and D. B. Spalding: Mathematical Models of Turbulence. Academic Press, London, 1972.

20. Harlow, F. H., ed.: Turbulence Transport Modeling. AIAA Selected Reprint Series, Vol. XIV, 1973.

21. Prandtl, L.: Bericht Uber Untersuchingen Zur Ausgebildeten Turbulenz. ZAMM, Vol. 5, 1925, p. 136.

22. Patankar, S. V. and D. B. Spalding: Heat and Mass Transfer in Boundary Layers. Intertext Books, London, 1970.

23. Maise, G. and H. McDonald: Mixing Length and Kinematic Eddy Viscosity in a Compressible Boundary Layer. AIAA Journal, Vol. 6, 1968, pp. 73-80.

24. McDonald, H. and F. J. Camarata: An Extended Mixing Length Approach for Computing the Turbulent Boundary Layer Development. Proceedings of the AFOSR-IFP-Stanford Conference on Boundary Layer Prediction, 1968.

25. Williamson, J. W.: An Extension of Prandtl's Mixing Length Theory. Applied Mechanics and Fluids Engineering Conference, ASME, June 1969.

26. Lilley, D. G.: Prediction of Inert Turbulent Swirl Flows. AIAA Paper No. 72-699, 1972.

27. Beer, J. M. and N. A. Chigier: Combustion Aerodynamics. Wiley, New York, 1972.

28. Walz, A.: Boundary Layers of Flow and Temperature. M.I.T. Press, Cambridge, Massachusetts, 1969.

29. Lavoie, G. A., J. B. Heywood, and J. C. Keck: Experimental and Theoretical Study of Nitric Oxide Formation in Internal Combustion Engines. Combustion Science and Technology, Vol. 1, 1970, pp. 313-326.

30. Zeldovich, Ya. B., P. Ya. Sadounikov, and D. A. Frank-Kamenetskll: Oxidation of Nitrogen in Combustion. Academy of Sciences of USSR, Institute of Chemical Physics, Moscow-Leningrad, 1947.

31. Bowman, C. T. and D. J. Seery: Investigation of NO Formation Kinetics in the Combustion Process: The Methane-Oxygen-Nitrogen Reaction. Emissions from Continuous Combustion Systems, Plenum Publishing Company, New York, 1972.

32. Caretto, L. S., L. H. Muzio, R. T. Sawyer, and E. S. Starkman: The Role of Kinetics in Engine Emission of Nitric Oxide. Combustion Science and Technology, Vol. 3, 1971.

33. Baulch, D. L., D. D. Drysdale, D. G. Horne, and A. C. Lloyd: Critical Evaluation of Rate Data for Homogeneous Gas Phase Reactions of Interest in High-Temperature Systems. Report No. 4 Department of Physical Chemistry, Leeds University, United Kingdom, December 1969.

34. Campbell, I. M. and B. A. Thrush: Reactivity of Hydrogen to Atomic Nitrogen and Atomic Oxygen. Trans. Faraday Soc. 64, Part 5, 1968, pp. 1265-1274.

35. Brinkley, S. R.: Computational Methods in Combustion Calculations, Combustion Processes, Section C. High Speed Aerodynamics and Jet Propulsion, Vol. 2, B. Lewis, R. N. Peace and H. S. Taylor, eds., Princeton University Press, Princeton, 1956.

36. Brinkley, S. R.: Calculations of the Thermodynamic Properties of Multi-Component Systems and Evaluation of Propellant Performance Parameters. Proceedings of the First Conference on Kinetics, Equilibrium and Performance of High Temperature Systems, A. S. Bahn and E. E. Zukoski, eds. The Combustion Institute, 1960, pp. 74-81.

37. Gouldin, F. C.: Role of Turbulent Fluctuations in NO Formations. Combustion Science and Technology, Vol. 9, 1974, pp. 17-23.

38. Libby, P. A.: On Turbulent Flows with Fast Chemical Reactions, Part I: The Closure Problem. Combustion Science and Technology, Vol. 6, 1972, pp. 23-28.

39. Gibson, M. M. and B. B. Morgan: Mathematical Model of Combustion of Solid Particles in a Turbulent Stream with Recirculation. Journal of the Institute of Fuel, December 1970.

40. Spalding, D. B.: Mathematical Models of Continuous Combustion. Emissions from Continuous Combustion Systems. Plenum Publishing Company, New York, 1972.

41. Wise, H., J. Lorell, and B. J. Wood: The Effects of Chemical and Physical Parameters on the Burning Rate of a Liquid Droplet. Fifth Symposium (International) on Combustion, The Combustion Institute, 1955.

42. Wood, B. J., W. A. Rosser, and H. Wise: Combustion of Fuel Droplets. AIAA Journal, Vol. 1, No. 5, May 1973.

43. Gosman, A. D. and F. C. Lockwood: Incorporation of a Flux Model for Radiation into a Finite-Difference Procedure for Furnace Calculations. Fourteenth Symposium (International) on Combustion, The Combustion Institute, 1973, pp. 661-671.

44. Chen, J. C.: Simultaneous Radiative and Convective Heat Transfer in an Absorbing, Emitting and Scattering Medium in Slug Flow Between Parallel Plates. AIChE Journal, Vol. 10, No. 2, March 1964.

45. Larkin, B. K. and S. W. Churchill: Heat Transfer by Radiation Through Porous Insulations. AIChE Journal, Vol. 5, No. 4, December 1959.

46. Hottel, H. C. and A. F. Sarofim: Radiative Transfer. McGraw-Hill, New York, 1967.

47. Zeldovich, Ya. B. and Yu. P. Raizer: Physics of Shock Waves and High-Temperature Hydrodynamic Phenomena, Vols. I and II. Academic Press, New York, 1966.

48. Siddall, R. G.: Flux Methods for the Analysis of Radiant Heat Transfer. Journal of the Institute of Fuel, June 1974, pp. 101-109.

49. Anasoulis, R. F. and H. McDonald: A Study of Combustor Flow Computations and Comparison with Experiment. EPA Report No. 650/2-73-045, December, 1973.

50. McAdams, W. H.: Heat Transmission. McGraw-Hill, New York, 1954.

51. Hadvig, Sven: Gas Emissivity and Absorptivity: A Thermodynamic Study. Journal of the Institute of Fuel. Vol. 43, April 1970, pp. 129-135.

52. Taylor, P. B. and P. J. Foster: The Total Emissivities of Luminous and Non-luminous Flames. International Journal of Heat and Mass Transfer, Vol. 17, 1974, pp. 1591-1605.

53. Cess, R. D.: The Interaction of Thermal Radiation with Conduction and Convection Heat Transfer. Advances in Heat Transfer, Vol. 1, Academic Press, New York, 1964.

54. Vincenti, W. G. and C. H. Kruger, Jr.: Introduction to Physical Gas Dynamics. Wiley, New York, 1965.

55. Traugott, S. C.: An Improved Differential Approximation for Radiative Transfer with Spherical Symmetry. AIAA Journal, Vol. 7, No. 10, October 1969.

56. MacCormack, R. W.: Numerical Solution of the Interaction of a Shock Wave with a Laminar Boundary Layer. Proceedings of the Second International Conference on Numerical Methods in Fluid Dynamics; Springer-Verlag, New York, 1971, p. 151.

57. Allen, J. S. and S. I. Cheng: Numerical Solutions of the Compressible Navier-Stokes Equations for the Laminar Near Wake. Physics of Fluids, Vol. 13, No. 1, 1970, p. 37.

58. Roache, P. J. and T. J. Mueller: Numerical Solutions of Laminar Separated Flows. AIAA Journal, Vol. 8, No. 3, 1970, p. 530.

59. Victoria, K. J. and G. F. Widhopf: Numerical Solution of the Unsteady Navier-Stokes Equations in Curvilinear Coordinates: The Hypersonic Blunt Body Merged Layer Problem. Proceedings of the Third International Conference on Numerical Methods in Fluid Dynamics, Vol. II; Springer-Verlag, New York, 1973, p. 254.

60. Douglas, J. and J. E. Gunn: A General Formulation of Alternating Direction Methods. Numerische Math., Vol. 6, 1964, p. 428.

61. Isaacson, E. and H. B. Keller: Analysis of Numerical Methods. Wiley, New York, 1966.

62. Peaceman, D. W. and H. H. Rachford: The Numerical Solution of Parabolic and Elliptic Differential Equations. J. Soc. Indust. Appl. Math., Vol. 3, 1955, p. 28.

63. Douglas, J.: On the Numerical Integration of $u_{xx} + u_{yy} = u_t$ by Implicit Methods. J. Soc. Indust. Appl. Math., Vol. 3, 1955, p. 42.

64. Mitchell, A. R.: Computational Methods in Partial Differential Equations. Wiley, New York, 1969.

65. Yanenko, N. N.: The Method of Fractional Steps, Translation edited by M. Holt. Springer-Verlag, New York, 1971.

66. Gourlay, A. R. and J. Ll. Morris: Finite-Difference Methods for Non-linear Hyperbolic Systems. Math. Comp., Vol. 22, 1968, p. 28.

67. Richtmyer, R. D. and K. W. Morton: Difference Methods for Initial Value Problems. Second Edition. Interscience, New York. 1967.

68. Roache, P. J.: On Artificial Viscosity. Journal of Computational Physics, Vol. 10, 1972, p. 169.

69. Roache, P. J.: Computational Fluid Dynamics. Hermosa Publishers, Albuquerque, New Mexico, 1972.

70. Roberts, G. O.: Computational Meshes for Boundary Layer Problems. Proceedings of the Second International Conference on Numerical Methods in Fluid Dynamics, Springer-Verlag, New York, 1971, p. 171.

71. Anderson, O. L.: User's Manual for a Finite-Difference Calculation of Turbulent Swirling Compressible Flow in Axisymmetric Ducts with Struts and Slot Cooled Walls. USAAMRDL-TR-74-50, Vol. I, 1974.

72. Briley, W. R. and H. McDonald: Computation of Three-Dimensional Turbulent Subsonic Flow in Curved Passages. United Aircraft Research Laboratories Report No. R75-911596-8, March 1975.